

AE No. 24 E
October 1990

R+D-Program Direct Disposal

Semi-Annual Report
01.07.1989 - 31.12.1989

with contributions by
Bundesanstalt für Geowissenschaften und Rohstoffe (BGR)
Deutsche Gesellschaft zum Bau und Betrieb von Endlagern
für Abfallstoffe (DBE)
Deutsche Gesellschaft für Wiederaufarbeitung von
Kernbrennstoffen (DWK)
Gesellschaft für Strahlen- und Umweltforschung (GSF)
Kernforschungszentrum Karlsruhe (KfK)
Siemens AG, UB KWU

Kernforschungszentrum Karlsruhe

9101220415 901218
PDR WASTE 412 PDR
WM-1

AE Reports

The Kernforschungszentrum Karlsruhe GmbH on behalf of the Federal Ministry for Research and Technology co-ordinates and attends to all repository relevant work undertaken in the framework of the direct disposal R+D program. It publishes the AE report series with the objective of communicating promptly the results of work performed to all participating in this programme.

It is not permitted to quote the contents of the AE reports. Prior to transmission of the reports and diffusion of their contents, respectively, the consent shall be obtained from the Projektgruppe Andere Entsorgungstechniken at the Karlsruhe Nuclear Research Center (KfK-PAE).

The authors and their institutions, respectively, assume responsibility for the contents. The Kernforschungszentrum Karlsruhe GmbH does not give a warranty, in particular not for the correctness, accuracy and completeness of information and for compliance with individual rights of third persons.

Printed and distributed by:
Kernforschungszentrum Karlsruhe GmbH
Postfach 3640, 7500 Karlsruhe 1
Printed in the Federal Republic of Germany

received with letter dtd. 12/18/90

R + D Program Direct Disposal

AE No. 24 E

Semi-Annual Report

**Reporting Period
July 1, 1989 - December 31, 1989**

**Compiled by
Projektgruppe Andere Entsorgungstechniken (PAE)
Using Contributions by
BGR, DBE, GNS, GSF, KfK, and UB KWU of Siemens AG**

**Kernforschungszentrum Karlsruhe
Projektgruppe Andere Entsorgungstechniken**

CONTENTS

1 INTRODUCTION	1-1
2 CASK DEVELOPMENT AND CONDITIONING TECHNIQUE	2-1
2.1 Cask Development	2-1
2.2 Pilot Conditioning Plant	2-3
2.3 Component Testing	2-4
3 DEMONSTRATION EXPERIMENTS ON DIRECT DISPOSAL	3-1
3.1 Thermal Simulation of Drift Emplacement (TSS)	3-1
3.2 Handling Tests for Drift Emplacement (HHV)	3-25
3.3 Simulation of Shaft Hoisting (SST)	3-27
3.4 Active Handling Experiments with Neutron Sources (AHE)	3-36
4 SYSTEMS ANALYSIS DUAL-PURPOSE REPOSITORY	4-1
4.1 Systems Evaluation and Future Program	4-1
4.2 Parameter Variations	4-2
5 EXPERIMENTAL INVESTIGATIONS	5-1
5.1 Corrosion Studies of Cask Materials	5-1
5.2 Retention of Gaseous Fission Products in the Backfill Material	5-5
5.3 Leaching Behavior of LWR Fuel	5-7
6 REFERENCES	6-1
7 ABBREVIATIONS AND ACRONYMS	7-1

CONTENTS

1 INTRODUCTION 1-1

1 INTRODUCTION

In its decision of January 23, 1985, the German Federal Government deemed it appropriate to further develop to the level of application the concept of direct disposal of spent LWR fuel elements in addition to pursuing the development of waste management with reprocessing. The contribution by the Federal Government in this case is restricted primarily to the area for which it is responsible under the German Atomic Energy Act, namely disposal. The further advancement of conditioning technology is a responsibility of industry, i. e., the utilities and GNS (DWK).

Advanced development work on the repository is coordinated by the Project Group Alternative Entsorgung*) (Projektgruppe Andere Entsorgungstechniken, PAE) established by the Karlsruhe Nuclear Research Center (KfK) on behalf of the German Federal Ministry of Research and Technology (BMFT). In addition, the Karlsruhe Nuclear Research Center spends part of its basic funds on activities designed to further develop direct disposal. Running the demonstration tests and planning the repository are responsibilities of Deutsche Gesellschaft zum Bau und Betrieb von Endlagern für Abfallstoffe, DBE. The Gesellschaft für Strahlen- und Umweltforschung (GSF) makes available the Asse experimental mine for some of the planned studies, in which it also participates. Also, the Federal Institute of Geosciences and Raw Materials (Bundesanstalt für Geowissenschaften und Rohstoffe, BGR) contributes to the ongoing activities. All projects are harmonized with the Bundesamt für Strahlenschutz (BfS).

Cooperation based on contracts exists between KfK and GNS/DWK. GNS/DWK is planning the construction of a pilot conditioning plant for spent fuel elements for direct disposal in Lower Saxony, close to the Gorleben exploratory mine; in this way, a continuous flow of information is ensured among the parties actively working on the repository and the conditioning technology side.

*) Entsorgung is a versatile German term that describes all steps at the back-end of the fuel cycle

The work planned for the next few years on direct disposal of LWR fuel assemblies is outlined in Part B of the "Research and Development Program on the Direct Disposal of Spent Fuel Elements from High Temperature Reactors and Light Water Reactors", published in May 1987. This semi-annual report summarizes the results of activities pursued in the second half of 1989. It has been compiled primarily to inform participants in the program and other interested parties of the progress of work on the direct disposal of LWR fuel assemblies. The report is arranged like the R&D program.

CONTENTS

2	CASK DEVELOPMENT AND CONDITIONING TECHNIQUE	2-1
2.1	Cask Development	2-1
2.1.1	Objectives and Schedule	2-1
2.1.2	Ongoing Work	2-2
2.1.3	Future Work	2-2
2.2	Pilot Conditioning Plant	2-3
2.2.1	Objectives and Schedule	2-3
2.2.2	Ongoing Work	2-3
2.2.3	Future Work	2-3
2.3	Component Testing	2-4
2.3.1	Objectives and Schedule	2-4
2.3.2	Ongoing Work	2-4
2.3.3	Future Work	2-5

2 CASK DEVELOPMENT AND CONDITIONING TECHNIQUE

2.1 Cask Development

2.1.1 Objectives and Schedule

To demonstrate the feasibility of pilot conditioning plant operation and of direct disposal, the following cask concepts have been developed:

- POLLUX cask for disassembled LWR fuel holding
 - 8 PWR uranium/recycle uranium fuel assemblies, medium burnup,
 - 24 BWR uranium/recycle uranium fuel assemblies, medium burnup.

- POLLUX cask for intact LWR/LMFBR fuel assemblies holding
 - 4 PWR uranium/recycle uranium fuel assemblies, high burnup,
 - 12 BWR uranium/recycle uranium fuel assemblies, high burnup,
 - mixed loading of BWR/PWR uranium/recycle uranium fuel assemblies, high burnup,
 - 3 PWR/10 BWR MOX fuel assemblies, high burnup.

- POLLUX cask for HTR fuel holding
 - 12,600 and 10,500 HTR fuel pebbles, respectively

- POLLUX cask for FBR assemblies

- POLLUX canister for chopped fuel rod sections holding
 - 0.5 PWR fuel assemblies,
 - 1.5 BWR fuel assemblies.

The packages of LWR fuel assemblies meet the repository storage criteria listed in the BMFT AET project (1980-1985) i. e., especially the control of mechanical forces arising from rock pressure and the required resistance to an assumed, though unlikely, attack by brine. By defining minimum decay times or periods of interim storage, packaging of fuel assemblies into these casks is so flexible that additional future aspects arising from repository planning can be taken into account, such as shielding, heat dissipation, etc.

The time schedule for the development of the cask system provides for the filing for permits under the Atomic Energy Act and under transport legislation after the first partial permit will have been granted to the pilot conditioning plant.

The appropriate permits must have been issued at the latest by the time the pilot conditioning plant will be started up, in order to ensure proper operation of that plant. (Hot commissioning of the pilot conditioning plant is scheduled for 1994).

2.1.2 Ongoing Work

Ultrasonic quality control of the cask lid welding seam.

In order to achieve 100% testing for imperfections of the welding seam the appropriate position of the ultrasonic testing device was defined and documented. By application of the ultrasonic technique at angles of 45°, 60°, and 70° in direct and indirect beam mode from the top of the POLLUX lid a non-destructive test and evaluation of the welding seam is feasible.

2.1.3 Future Work

A prototype POLLUX 8 PWR/24 BWR is being fabricated. End of 1990 it should be available for handling experiments.

The safety reports for a license for POLLUX casks according to the Atomic Energy Act and transport regulations are to be handed to the authorities, and the respective licenses are to be applied for in 1990.

2.2 Pilot Conditioning Plant

2.2.1 Objectives and Schedule

Supplementary to reprocessing, also direct disposal of spent fuel assemblies is to be developed further. Suitable processes are to be developed, tested and demonstrated in the pilot conditioning plant.

The following schedule has been envisaged:

Construction of the facility from 1990 to	1994
Commissioning in	1994.

2.2.2 Ongoing Work

2.2.2.1 Status of the licensing procedure

The documents for the licensing procedures according to the Atomic Energy Act and other regulations were reviewed to meet the requirements of the experts' evaluations. At the end of the year all final expertises were available, the licenses are expected for beginning of 1990.

2.2.2.2 Status of Planning

The erection of safety relevant components (fences, walls etc.) was promoted by planning and application for license.

2.2.3 Future Work

- Opening of the building site in order to erect safety relevant components
- Placing the order for erection of the pilot conditioning plant
- Beginning the preparation of documents for the second partial license of the pilot conditioning plant.

2.3 Component Testing

2.3.1 Objectives and Schedule

While the facility is being planned, some of the main components for fuel assembly conditioning are being tested and optimized. The purpose of the exercise is to confirm the operating principle, verify the conceptual design, and back up the licensing procedure. Testing the main components is to be completed by the end of 1990.

2.3.2 Ongoing Work

2.3.2.1 Fuel Assembly Hardware Compaction Device

The compaction experiments with the compaction device were continued with pre-disassembled hardware and with cladding imitate. The envisaged length of the compacted blocks of 550 mm was already attained at a compaction force far below 5,000 kN. Two steel cans filled with cladding imitate were compacted at maximum compaction force. These compacted cans were consecutively sawn apart in order to investigate their inner structure. It turned out that the compaction process did not occur uniformly. The maximum density was observed at the circumference i.e. along the guided surfaces. Further compaction tests are not intended.

2.3.2.2 Fuel Assembly Disassembling

Further tests were performed with the experimental device to disassemble fuel assemblies. In particular brackets to fix fuel assemblies of PWR and BWR were tested, as well as cutting tools and a vibrator to align pin bulks.

2.3.2.3 Fuel Pin Shear

The fuel pin shear was attached to the already existing test rig for POLLUX canister loading. The device was designed such that after the insertion of a fuel pin cutting and loading of pin segments into the canister proceeds automatically. The cutting tool was tested successfully in a series of more than 1,000 cuts.

2.3.2.4 Reloading of THTR fuel pebbles

A test rig to convey pneumatically THTR fuel pebbles was erected at the DWK test site at Lahde. By means of a suction ventilator fuel pebbles were conveyed out of a POLLUX cask into another container. It took about 20 minutes time to convey 3,000 pebbles. Interim storage canisters of THTR and AVR were emptied the same way.

2.3.3 Future Work

The fuel assembly disassembling device will be changed such that it can handle also fuel assemblies different from the standard type. The tests to push the bulk of individualized pins into the POLLUX can must be repeated due to changes carried out at the can in order to improve heat removal. This will be concluded middle of 1990.

CONTENTS

3	<i>DEMONSTRATION EXPERIMENTS ON DIRECT DISPOSAL</i>	3-1
3.1	Thermal Simulation of Drift Emplacement (TSS)	3-1
3.1.1	Objectives and Schedule	3-1
3.1.2	Ongoing Work	3-2
3.1.3	Future Work	3-24
3.2	Handling Tests for Drift Emplacement (HHV)	3-25
3.2.1	Objective and Schedule	3-25
3.2.2	Ongoing Work	3-25
3.2.3	Future Work	3-26
3.3	Simulation of Shaft Hoisting (SST)	3-27
3.3.1	Objective and Schedule	3-27
3.3.2	Ongoing Work	3-27
3.3.3	Future Work	3-35
3.4	Active Handling Experiments Using Neutron Sources (AHE)	3-36
3.4.1	Objectives and Schedule	3-36
3.4.2	Ongoing Work	3-36
3.4.3	Future Work	3-46

3 DEMONSTRATION EXPERIMENTS ON DIRECT DISPOSAL

3.1 Thermal Simulation of Drift Emplacement (TSS)

3.1.1 Objectives and Schedule

The reference concept of direct disposal of spent fuel assemblies is based on conditioning fuel rods in self-shielding casks (POLLUX casks) and storing those casks in the drifts of a mined geologic repository. The drifts will be backfilled with crushed salt immediately after emplacement. A POLLUX cask is 1.5 m in diameter, 5.5 m in length, and it weighs up to 65 t. It contains the fuel rods and compacted disassembly hardware of up to eight PWR-fuel assemblies (corresponding to 4.27 t of uranium) which, depending on the period of interim storage prior to emplacement, generate up to 7.5 kW of heat. For a permit to be granted this concept requires demonstration of safe handling, transport and emplacement of the casks in the repository.

The "Thermal Simulation of Drift Emplacement" demonstration test contributes to proving safe disposal of spent fuel. It serves to study the characteristics and the behaviour of the backfill material surrounding the casks and of the rock under the influence of heat. The measured data are compared with results of thermal and thermomechanical forecasting calculations in order to validate the codes and models used for calculation. Another objective of the experiment is to demonstrate a suitable method of backfilling the drifts with crushed salt.

In a previous experiment, the two possible methods of backfilling (pneumatic and by means of a sling belt) were tested under realistic conditions, but without the casks being heated. On the basis of this experiment, the sling belt method was considered most suitable for the main experiment.

For the main experiment, two parallel drifts, each 70 m long, approx. 14 m² in cross section and spaced 14 m apart (pillar thickness 10 m), were excavated 800 m below the surface at the Asse salt mine. Three heated test casks will be installed in each drift, their axial distance being 3 m. These test casks correspond to the POLLUX casks planned for direct disposal with respect to size, weight, and heat generation. The remaining empty space in the drifts will be

backfilled with crushed salt after the test casks and the measuring and control instruments have been installed.

For geotechnical studies, a system of boreholes were drilled in the rock around the test drifts for installation of measuring systems. Measurement boreholes were also drilled from drifts at the 750-m-level above the test drifts. The total length of all measurement boreholes will be approximately 2,700 m. Some of these boreholes were completed and instrumented even before the test drifts were excavated; in this way, also the impacts on the rock arising from drift excavation can be assessed.

The previous experiment and the conceptual planning of the main experiment were completed by mid-1987. Test field excavation was completed in 1989. The main experiment is due to begin in summer 1990 and has been planned for an initial period of three years. However, the technical components are designed in such a way that the experiment may be extended by another three years, if necessary, to allow rock mechanical and thermomechanical events in the test field to be measured over a prolonged period of time.

The demonstration test is carried out by BGR, DBE, GSF and KfK and is sponsored by the BMFT.

3.1.2 Ongoing Work

3.1.2.1 Survey

Excavation of drifts and boreholes within the test field was completed. The geological map of the test field shows that the test drifts are completely in the Main Salt Na2B.

The boreholes are almost completely equipped with monitoring devices. The measurement program for investigation of the condition of the rock during drift excavation and prior to heating was continued. Data are being collected by the data acquisition equipment.

The heater casks were delivered and are ready for installation. The electricity supply system entered service. The backfilling equipment was prepared for operation. An electronic bucket-loader weighing machine for measuring the amount of backfill in the drifts was calibrated. In order to analyze the condition of the backfill prior to emplacement, sampling was done of gases from the crushed salt pile.

Development of the gamma-probe for backfill density measurements at temperatures up to 200°C was completed. The final report is under preparation. The equipment for calibration of the probe is available.

3.1.2.2 Gas Measuring Program

A measuring program will be conducted in the whole test period in which degassing of the salt rock, volatile components from reactions between salt and casks as well as gases from thermal degradation will be investigated. For that purpose gas samples will be taken from the pore space in the backfill at twelve locations, i.e. three at the floor, at the mid plane, at the top of the casks and below the roof of the test drift. The required equipment was purchased and, as far as possible, installed.

Crushed rock from test drift excavation is being stored at several locations in the Asse salt mine. This material will be used for backfilling the test drifts following heater cask installation. In order to determine degassing of the backfill at room temperature, sampling was provided for at eight locations.

For this purpose glass filters were installed in the crushed salt. Sampling was carried out via teflon hoses by means of a hand suction pump in the time period from October 1989 to January 1990. Additionally samples were taken at four different locations in front of and above the crushed-rock piles. The samples were analyzed by gas chromatography relevant to their contents of hydrocarbons C₁-C₄, CO₂, CO, H₂S, SO₂ and HCl.

The composition of these gas samples is not significantly different from the composition of the mining air which has the following contents of the gases mentioned above:

- CH₄ between 0 and 5 vpm
- CO₂ between 300 and 800 vpm
- CO below 5 vpm
- H₂S below experimental detection limit
- SO₂ below experimental detection limit.

Fig. 3.1-1 shows CO₂-contents in the mining air in the test field. The variations probably were caused by ventilation and by diesel engines of mining vehicles. This was not analyzed in more detail. The volatile components from the rock salt obviously had escaped in the mining, sieving, and storing processes.

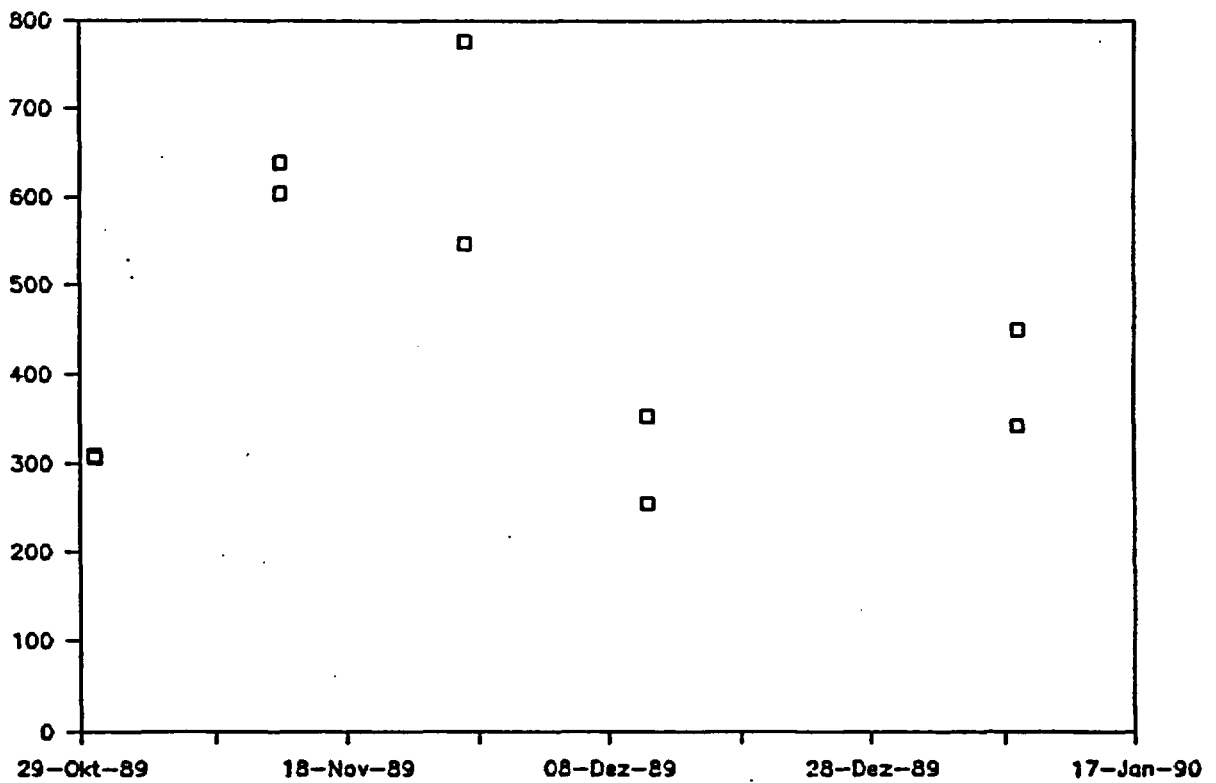


Fig. 3.1-1: CO₂-contents of the air in the test field

In addition to the in-situ investigations of the natural and thermally induced gas release, the chemical-mineralogical composition of the backfill and the temperature dependent gas release will be determined from about 30 representative backfill samples. For this purpose, during backfilling samples of 10 kg each will be taken at intervals of about 5 m of the backfilled drift.

In the drifts on the 750-m-level, 50 m above the heated test drifts, a large number of boreholes were drilled prior the excavation of the test drifts on the 800-m-level. In one of these boreholes (ÜF 20) a strongly malodorous atmosphere was detected in a pilot measurement. Steel was tarnishing rapidly. Three days after that pilot measurement gas samples were taken from 5.25 m and 40 m depth via teflon hose by means of a membrane pump. This measurement revealed an air-like atmosphere in the borehole containing 450 vpm CH₄, 10-15 vpm He, 1,000 vpm CO₂ and about 100 vpm of an up till now not identified gas component. However, these results are not representative, since the borehole was not closed gas-tight and the atmosphere was disturbed intensively by the pilot measurement three days before. For further investigations the borehole was plugged gas-tight and will not be disturbed over a longer period of time. Thus, equilibrium concentrations of the different gases can develop. In addition to the gases mentioned above brine accumulated in this borehole.

In a similar borehole 50 m apart (ÜF 23) neither brine nor a malodorous smell was detected. By analysis of a gas sample taken from 40 m depth air with contents of 300 vpm H₂, 20 vpm CH₄, and 640 vpm CO₂ was found. The unidentified component of borehole ÜF 20 was missing.

3.1.2.3 Geoscientific studies by the BGR

Structural and engineering geology investigations

The geological mapping of the test field was completed. It provides the basis for interpreting the measurement results and the special engineering geological data recorded parallel to the tests.

Lithology and structure of the salt rock surrounding the test drifts is illustrated in figure 3.1-2. The test drifts are located slightly north of the main Asse anticline within the upper "Stassfurt Main Salt" Na2B. In the near field of the test drifts the Stassfurt Main Salt forms a typically monotonous sequence of halite and anhydrite, dipping slightly to the southeast.

The orientated recovery of cores provide considerably greater petrographic and structural details when analyzed using a newly developed fluoroscopic screen; present in a matrix of for the most part fine crystalline, slightly contaminated halite there are "floating" fragments of large layered halite crystals and thin anhydrite beds. These reflect the original texture, but also exhibit in part extreme deformation, e.g. crumpling and shearing. In the primary halite crystals in particular there are a great number of micro-cracks. These are predominantly in an approximately normal orientation to the axis of drilling and are interpreted as discing due to pressure release. There are also, however, zones where strong deviations to this orientation are observable. The frequency distribution and spatial orientation of the cracks is currently being subjected to intensive statistical analysis; there is possibly a link between the primary stress field of the rock mass and the occurrence of these cracks. This analysis would not have been possible without orientated core recovery.

Rock mechanical investigations

In 1989 the following rock mechanical investigations and work were carried out:

- continuation of long-term stress measurements at the 750-m-level (overpass drift) with monitoring stations in boreholes Bo24 to Bo27,
- installation of additional stress monitoring stations and an additional data collection unit at the 800-m-level,

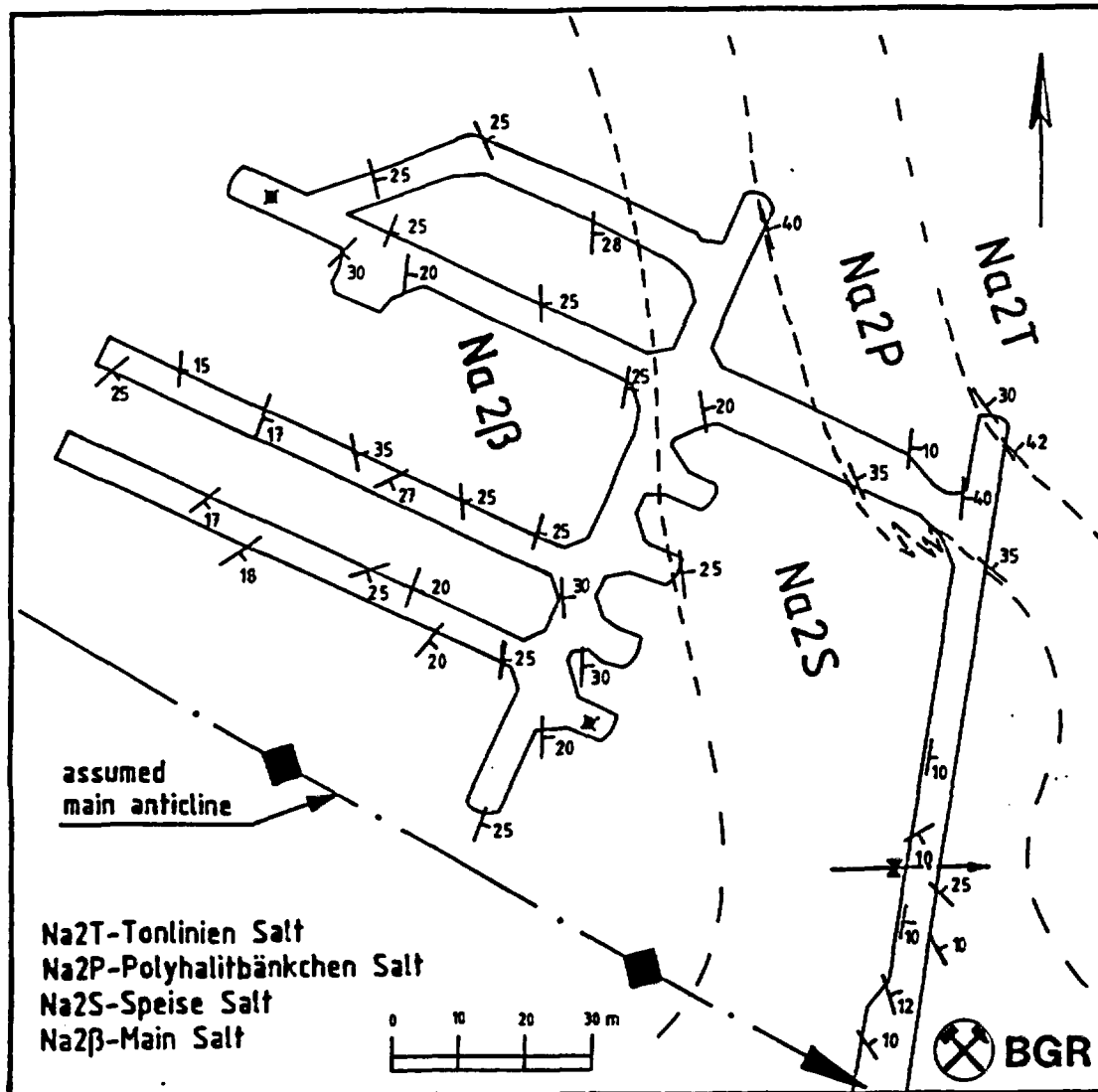


Fig. 3.1-2: Geological map of the PAE-TSS field at 800-m-level

- measuring stress changes during heading of test drifts A and B,
- execution of two slot cutting tests in test drift A,
- installation of large flat jacks in the slots,
- execution of rock mechanical laboratory tests on saltcrete.

Boreholes Bo29, Bo30 and Bo34 to Bo36 (see fig. 3.1-3) were fitted with 4-component stress monitoring stations with hydraulic pressure cells at various installation depths and orientations. Installation and pre-stressing techniques correspond to the methods used previously in the overpass drift. The data is registered at an additional automatic measuring station, installed in container cut CN2. The data measured in 1989 are typified by monitor station S30.3 in fig. 3.1-4 and monitor station S34.2 in fig. 3.1-5. Clear stress changes

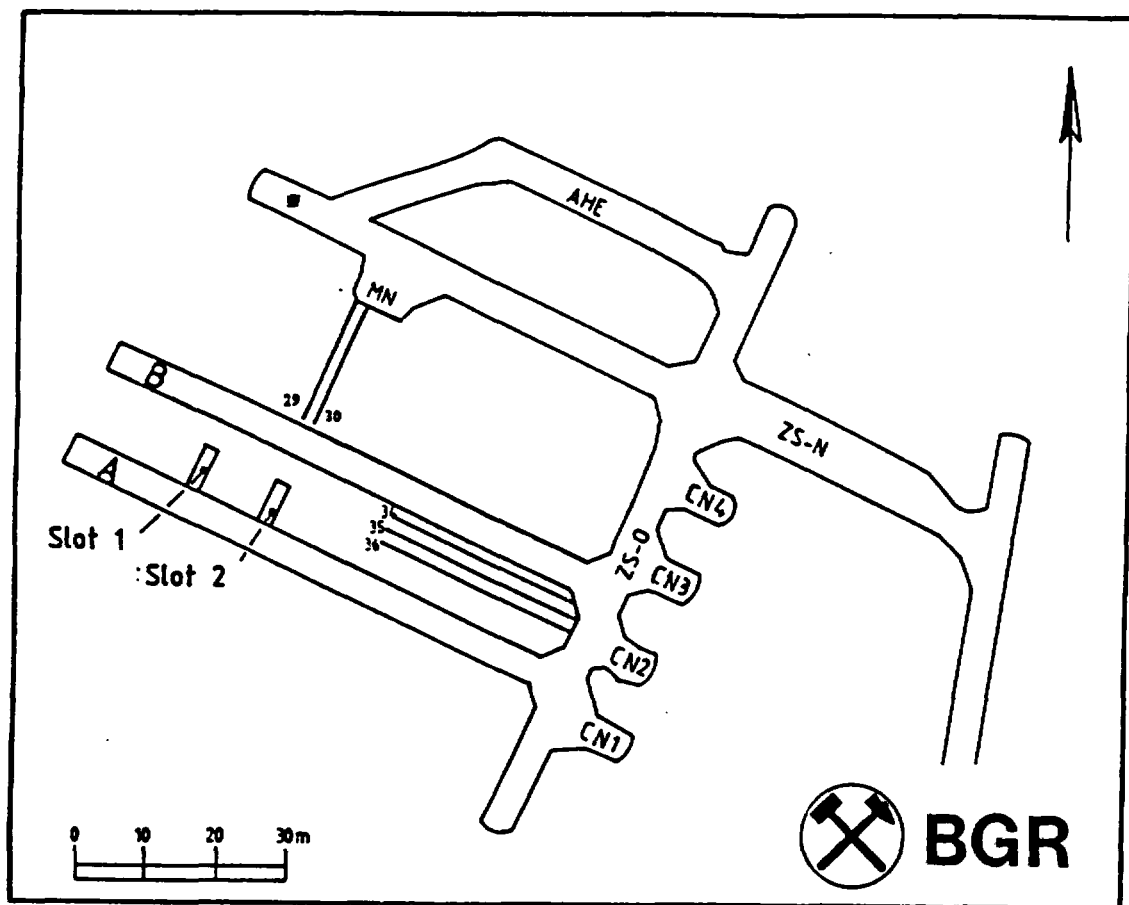


Fig. 3.1-3: Configuration of BGR boreholes and slots equipped in 1989 (800-m-level)

arose during the heading of test drift B during April 1989. The vertical and sub-vertical pressure cells showed the greatest stress changes.

In order to determine the stress gradients in the pillar between test drifts A and B two large-slot stress release tests were carried out using the BGR method /3-1/. The location of the slots is given in Fig. 3.1-3. To measure the stress release deformations two measuring boreholes were drilled per slot at 25 cm and 50 cm distance from the slot plane. The vertical stress release deformations occurring during the slotting of these boreholes are typified in fig. 3.1-6 and 3.1-7 as functions of slot advance. With the help of concurrent numerical calculations it is possible to use the stress release curves to derive the stress pattern in the drift zone /3-1/.

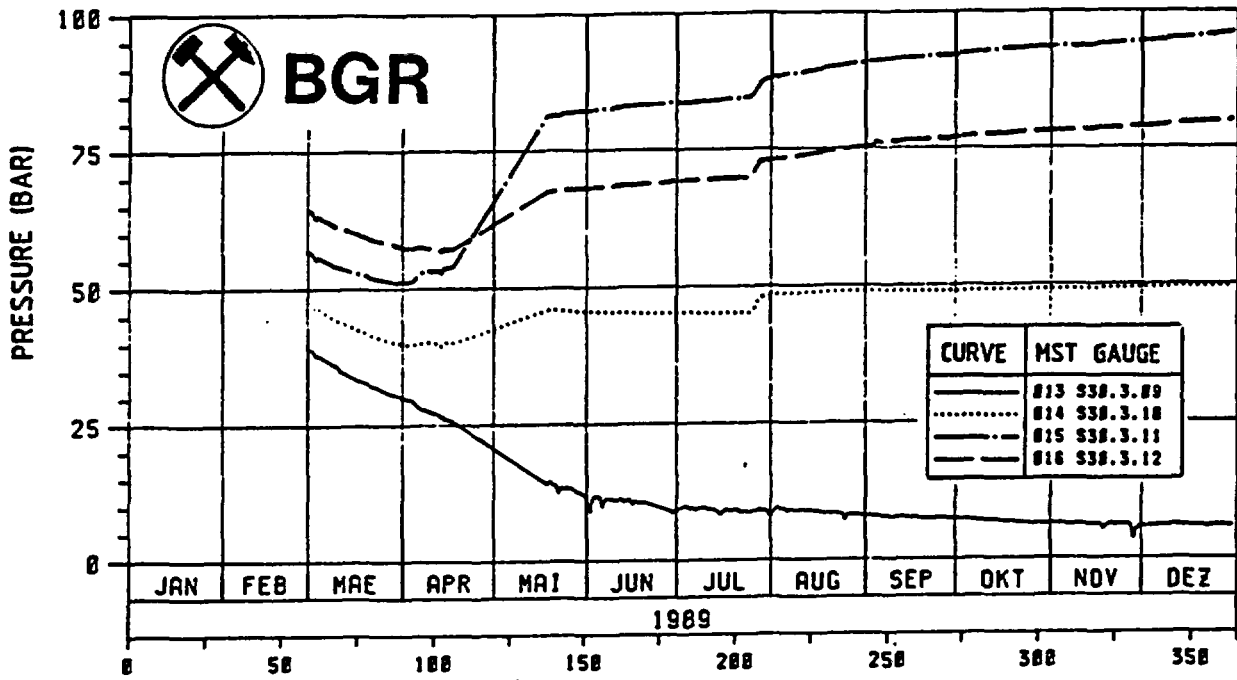


Fig. 3.1-4: Stress changes at monitor station S30.3

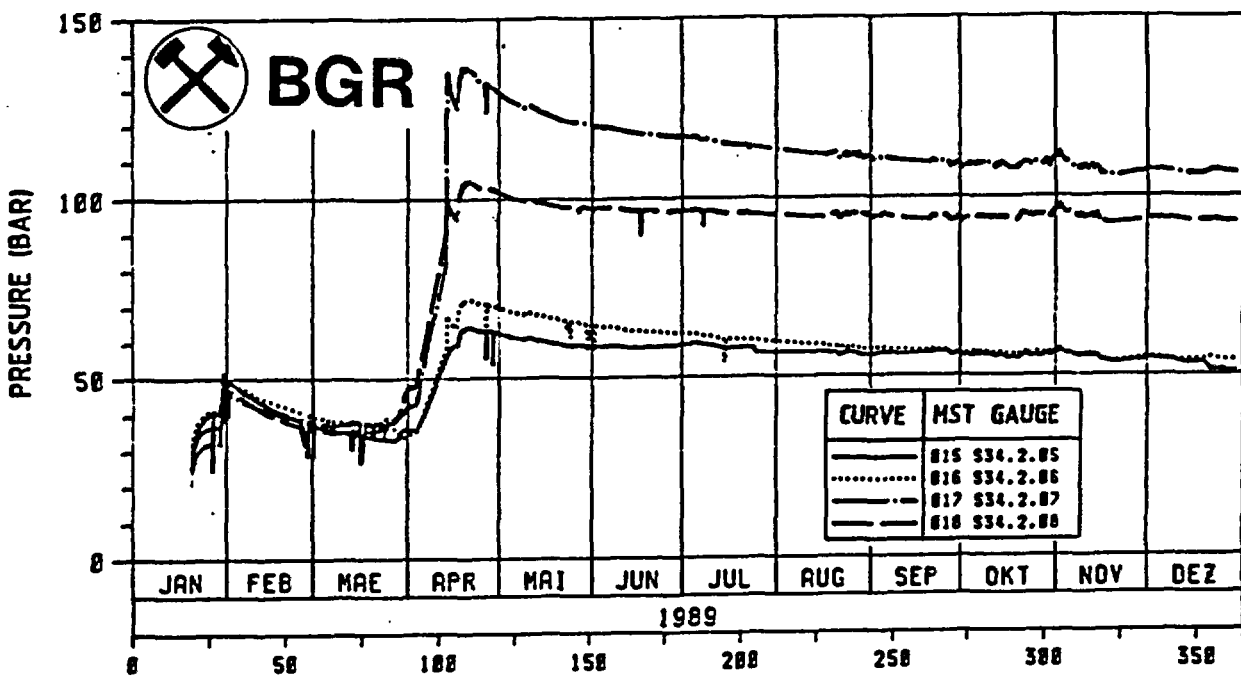


Fig. 3.1-5: Stress changes at monitor station S34.2

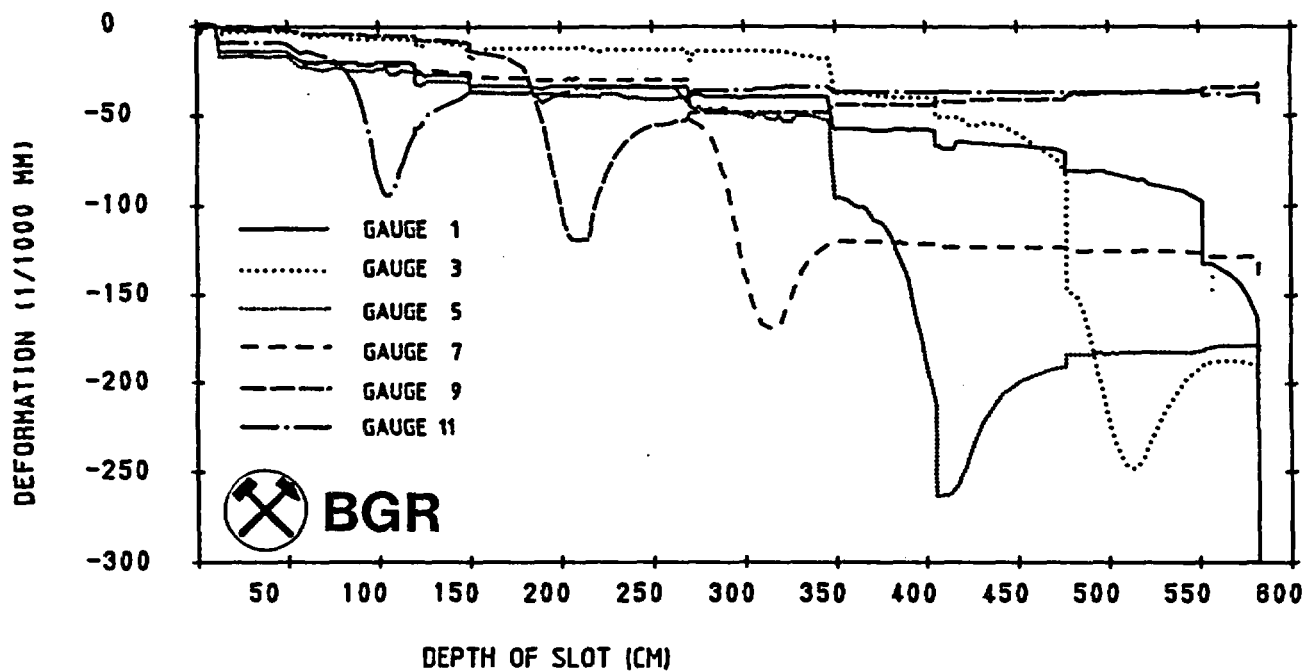


Fig. 3.1-6: Vertical stress release deformations during slot advance (measuring borehole 1; 25 cm below the slot)

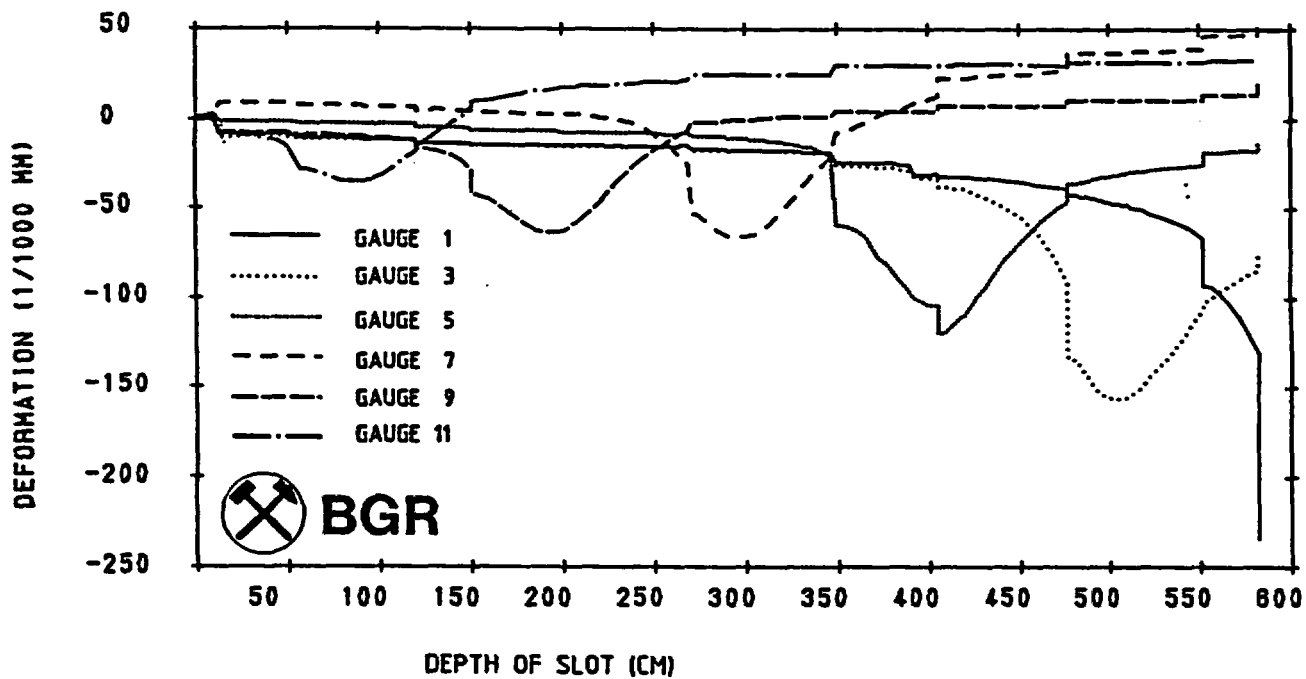


Fig. 3.1-7: Vertical stress release deformations during slot advance (measuring borehole 2; 50 cm below the slot)

After cutting of the slot 5 large flat jacks were installed in each slot together with temperature and pressure gauges to allow long-term measurements. The initial pressure buildup in the jacks due to convergence of the slots was measured manually at first in 1989 using manometers.

Following up this work laboratory tests were carried out on a biaxial test rig to determine the material properties of saltcrete. This saltcrete, a mix of brine, salt and magnesite, is used to backfill the measurement boreholes and slots. The first test results show that the mix chosen has a stiffness approximately equivalent to that of halite.

Geotechnical permeability studies

To determine the permeability of the salt rock and the backfill material around the test casks a number of vacuum measurements were carried out in 1989. Using a newly developed apparatus /3-2/ permeability was measured in four boreholes (Bo31, Bo32, Bo33 and Bo40). Thus reference measurements were completed in all boreholes currently available. Borehole 28 was tested in 1988 using a device with double packers. The borehole sections were generally separated by an approximately 1 m long pneumatic packer. At start of test the air pressure was approximately 10 mbar if the surrounding salt mass was relatively impermeable. Over a period of several hours (generally 20 hours) the subsequent pressure rise was observed. To standardize the results the average pressure rise factor was calculated in mbar per 1-m-borehole length unit. The results gained for borehole 40 (approx. 36 m long) are typical and are shown in fig. 3.1-8. With the exception of borehole 33, all boreholes show similar test results.

Relatively large permeabilities were measured in borehole 33. They can be explained by the deepest part of the borehole having only a minor distance to the floor of test drift B or possibly by a rough borehole surface. Future measurement campaigns, to be carried out at regular time intervals, will provide additional data.

To assess the test results finite element calculations were carried out taking into account the gas flow using the GM88 (gas model) /3-3/ program. GM88 is a component of the 3D DURST program system developed during BMFT pro-

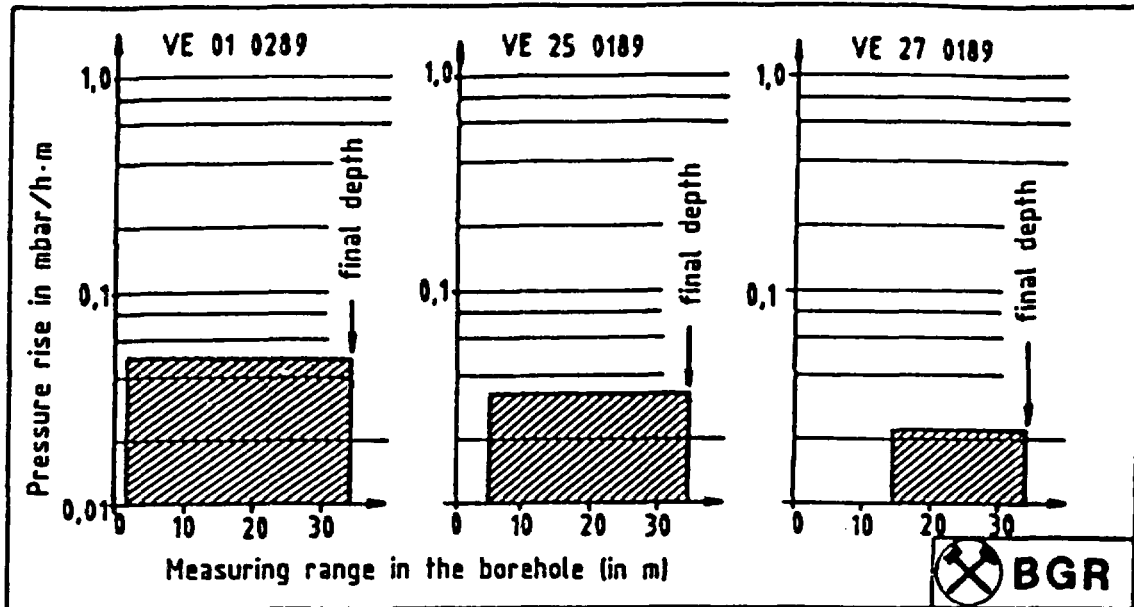


Fig. 3.1-8: Pressure rise measured in borehole 40

ject "Fracture System Flow Test" /3-4/. To calculate the pressure in spatial gas flows in a rock mass the continuity equation for ideal gases was applied together with Darcy's law, i.e. gravity and rock compressibility were neglected. The calculation was carried out using a quarter section model with 16 macro elements, in which the centre was taken as source. Density and pressure curves of the gas in the rock, in particular time dependent changes of the pressure curves for storage coefficient $S = 0.01$, were calculated assuming a homogeneous rock matrix.

3.1.2.4 Geoscientific studies by the GSF

a) Studies from the overpass drift at the 750-m-level

At the 750-m-level mining activities were completed at the end of year 1988, installation and commissioning of the instruments was completed early 1989. Since that time the deformations between the 750-m-level and the 800-m-level is monitored by extensometers, inclinometers and convergence lines. In order to accelerate contact between hydraulic flat jacks and sensors a reinjection of the stress monitoring stations was performed.

Rockmechanical reactions resulting from test drift excavation at the 800-m-level were monitored by stress- and deformation sensors.

Temperature measurement

In order to monitor rock temperatures between 750-m and 800-m-level, thermocouples were installed in the deformation - and stress measurement boreholes. Since April 1988 in this region temperatures between 35°C and 37°C were measured. As an example results of measurements in borehole 7 are shown in fig. 3.1-9. Significant temperature changes outside the measuring detection limit of the sensors were not measured.

Temperature differences can be explained by the natural temperature gradient of about 3°C/100 m. Therefore, temperatures measured at 14,5 m depth are lower than temperatures measured at greater depths.

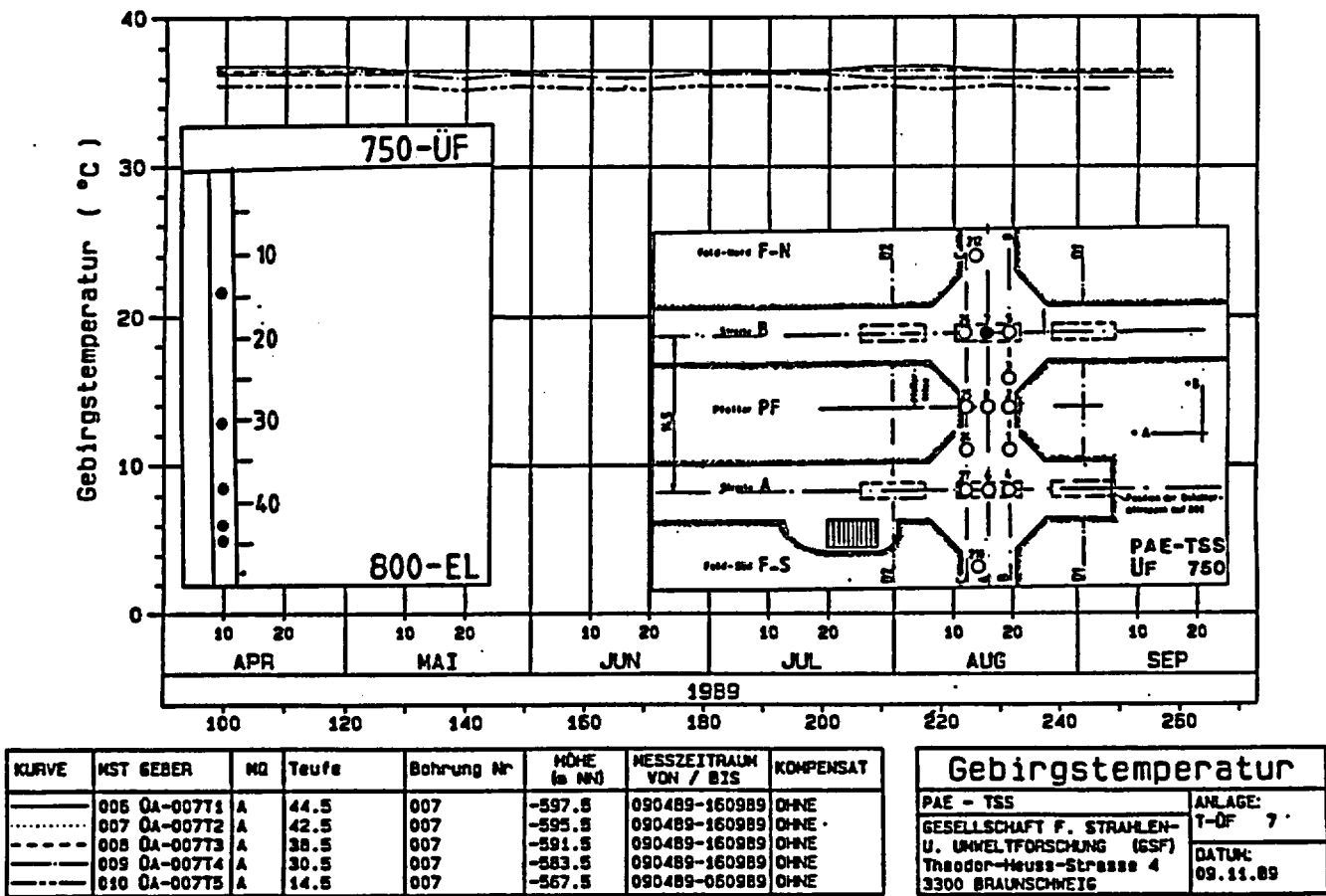


Fig. 3.1-9: Temperatures measured in borehole 7. Shown are also positions of boreholes from the overpass drifts

Inclinometer measurement

By inclinometer measurements the borehole slopes in two perpendicular directions are recorded. For guidance of the probe a plastic tube was cemented in the borehole. The tube wall contains two pairs of notches at angles of 90°. From the slope deviations two orthogonal components of the deformation vector are calculated.

For inclinometer measurements in the TSS test five boreholes 131 mm in diameter were drilled in section A + 1. Borehole 211, 65.6 m long, is in the center of the pillar between the test drifts. Boreholes 208 and 209, 45 m long, are drilled above the centerline of the test drifts, and boreholes 210 and 212, 65.5 m long, are outside the test drifts (see also fig. 3.1-10 and 3.1-11).

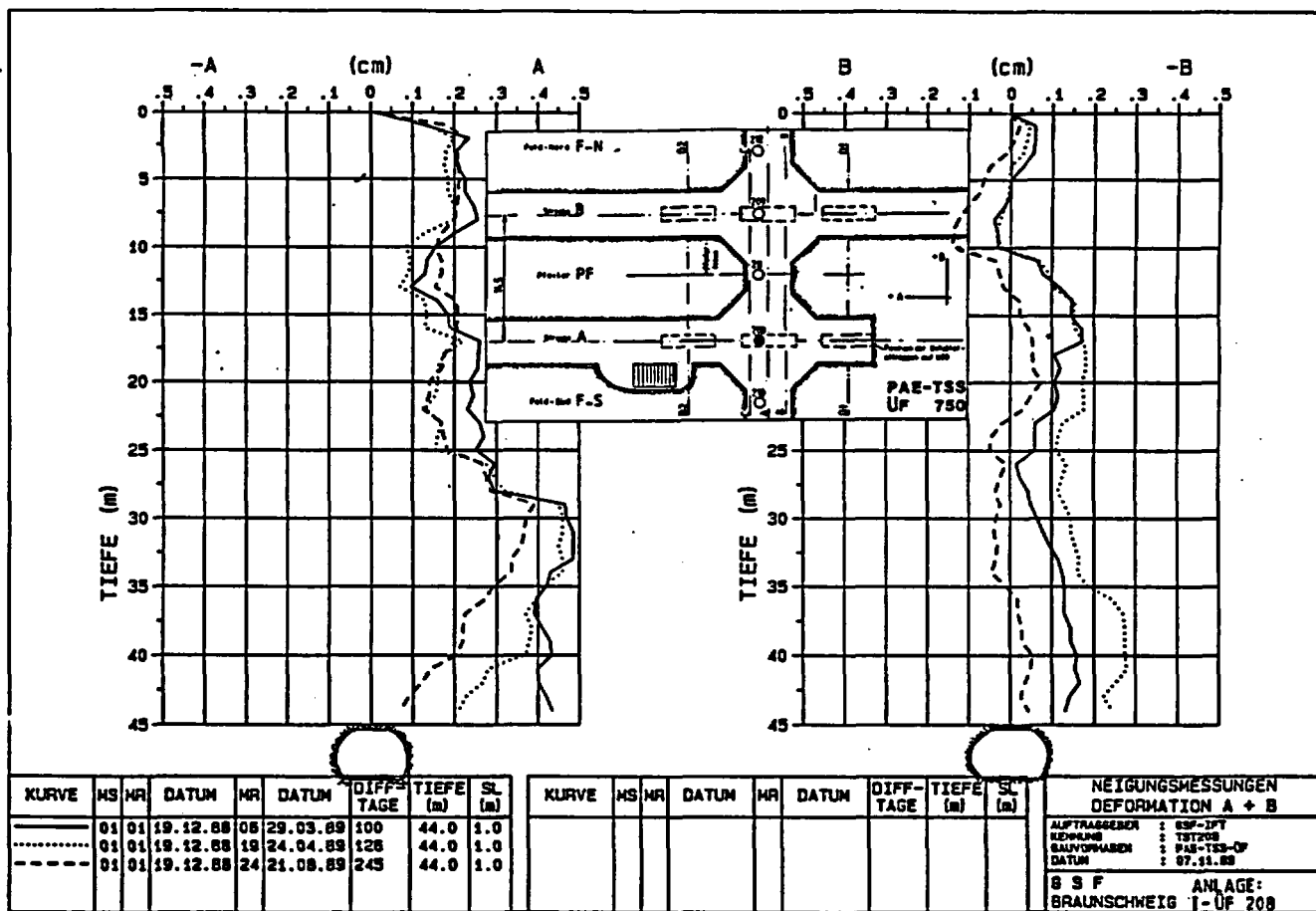


Fig. 3.1-10: Inclinometer measurements in borehole 208: deviations vs. borehole depth

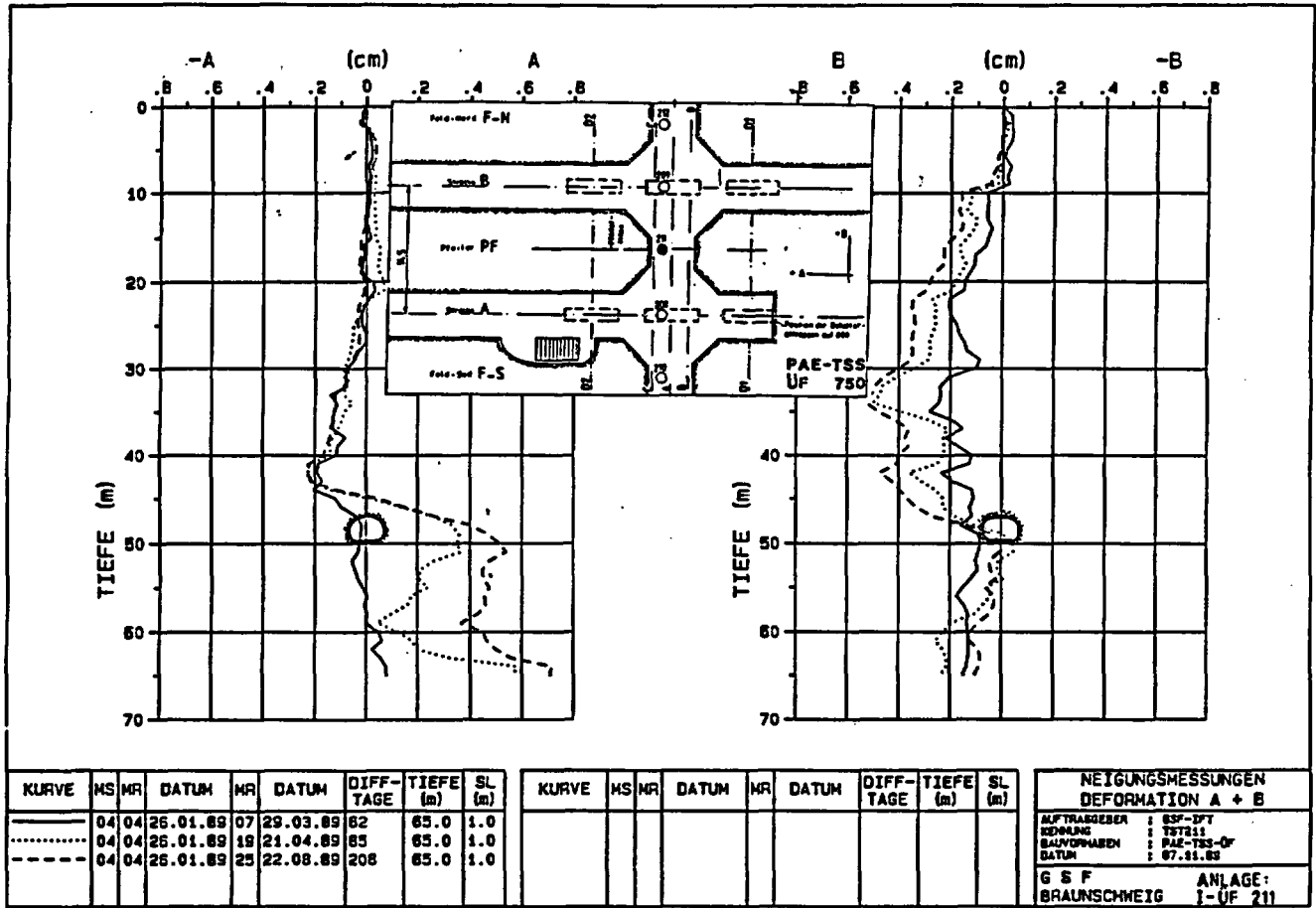


Fig. 3.1-11: Inclinometer measurements in borehole 211: deviations vs. borehole depth

Since December 1987 slopes are measured in boreholes 208 to 212. Deformations in boreholes 208 and 211 calculated from these measurements can be seen in figures 3.1-10 and 3.1-11.

Drift excavation near to the inclinometer boreholes was carried out from end of March to end of April 1989. It caused displacements both perpendicularly and parallel to the drift centerlines. One reason for displacements parallel to the drift axes is the temporal difference between excavation of both drifts.

Moreover, local deformation behavior is influenced by global deformations in the mine. Especially the neighbourhood of the test field to old carnallite excavations can be important. For quantification of these effects future measurements have to be observed.

Extensometer measurement

In order to measure longitudinal displacements of discrete locations in a borehole, in three boreholes of section A (fig. 3.1-9) multiple rod extensometers were installed. Borehole 8 (in the pillar) contains eight anchor points at 65 m depth. Boreholes 5 and 6 (above the test drifts) are equipped with five-point-extensometers. Anchor point positions of the extensometers are shown in figures 3.1-12 to 3.1-14.

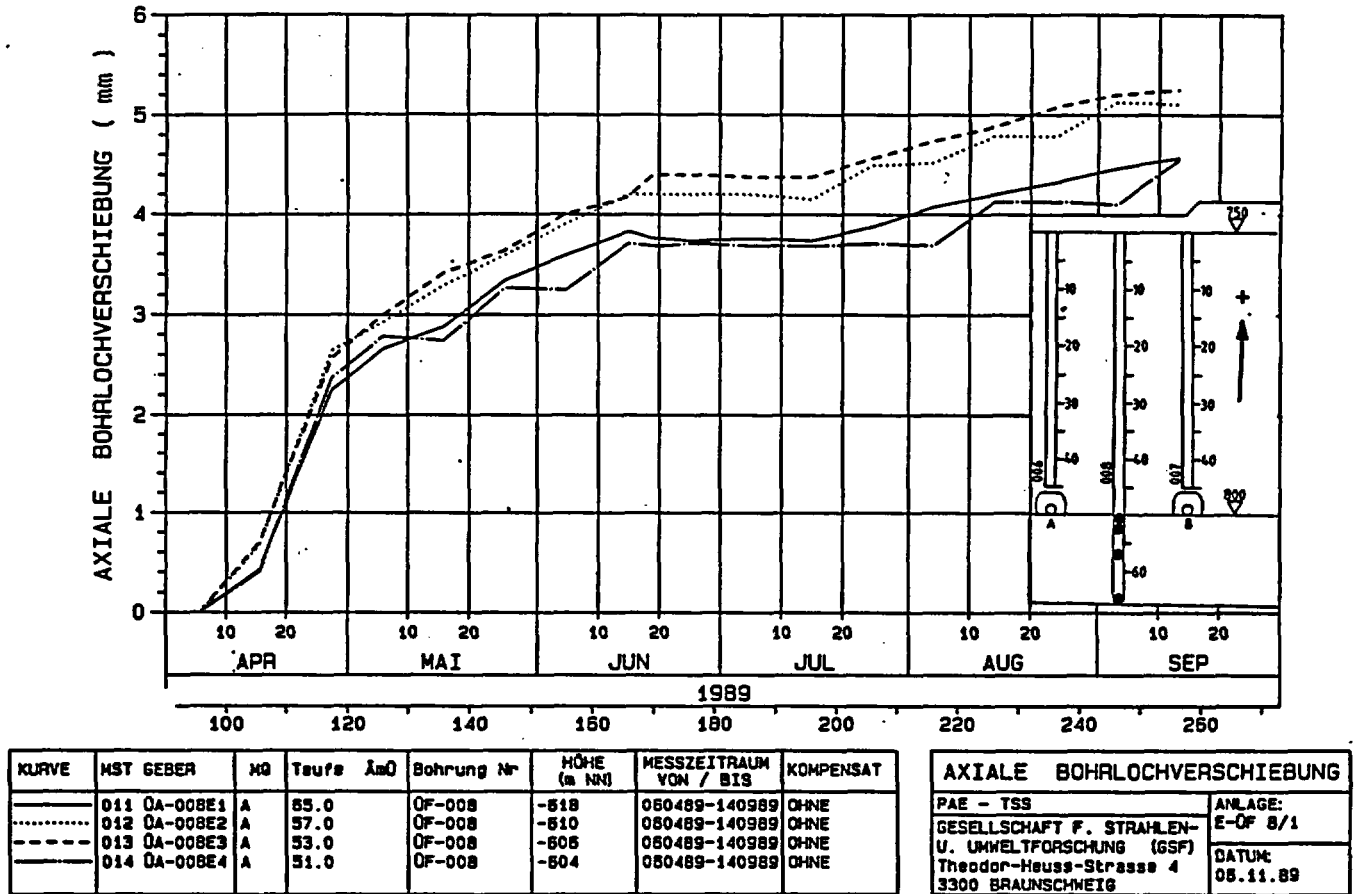


Fig. 3.1-12: Longitudinal displacements in borehole 8 below test drift level

Examples of displacements measured can be seen in figures 3.1-12 to 3.1-14. Drift excavation beginning at the end of March 1989 caused significant displacements proportional to the distance of the anchor points to the drifts. Extensometer 008 (in the pillar) shows upward movements for anchor points below the 800-m-level and downward movements for anchor points above the 800-m-level. By the extensometers above the test drifts downward displacements were measured. This means, that in all the measurements the ex-

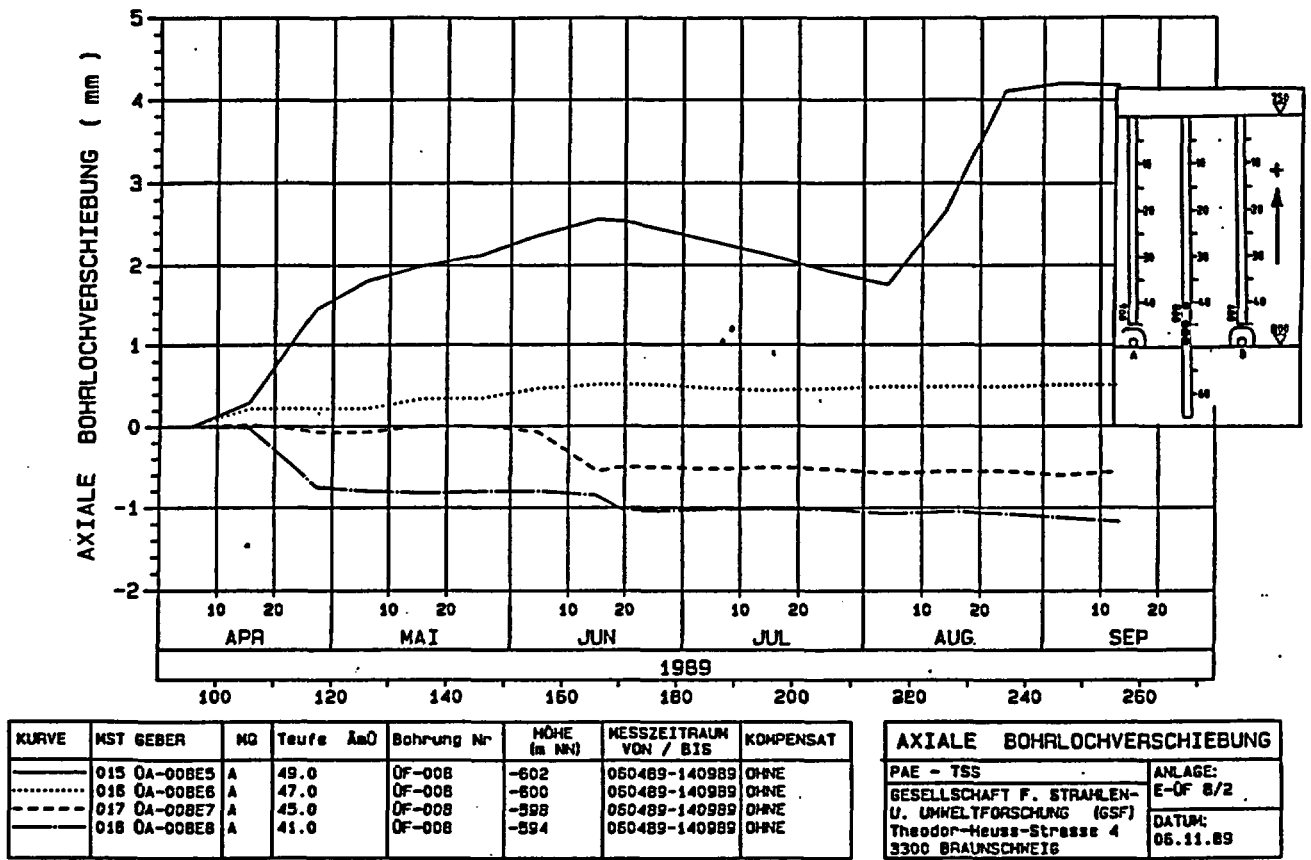


Fig. 3.1-13: Longitudinal displacements in borehole 8 above test drift level

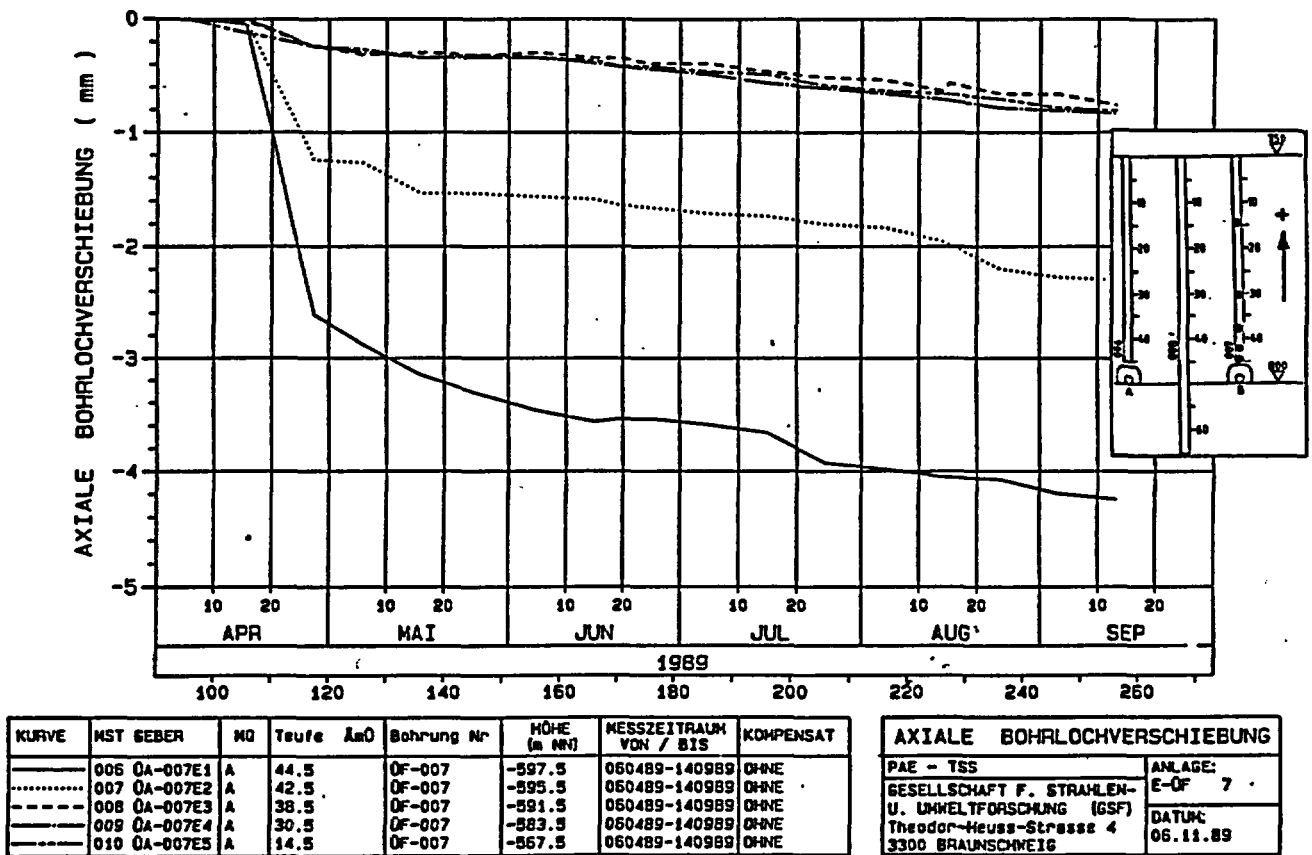


Fig. 3.1-14: Longitudinal displacements in borehole 7

pected convergence into the excavated drifts were monitored. The largest displacement of 1.3‰ were monitored by extensometer 007 in the 1.5 m long measuring section near to the drift.

Rock stress measurement

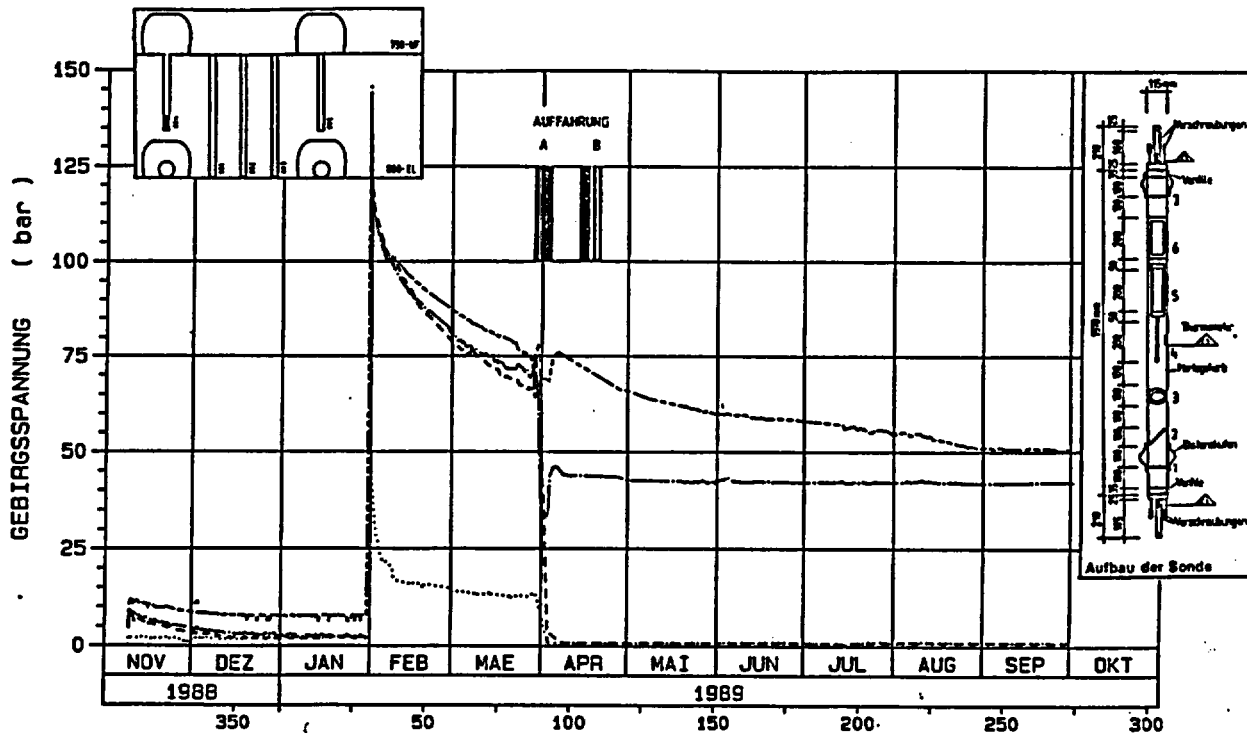
Stress monitoring stations were installed in boreholes 1 to 5 (see figure 3.1-9). They consist of seven hydraulic pressure cells, allowing recording of all six components of the spatial stress field. In order to measure the gradient along the monitoring station, vertical stresses are measured twice, at the top and the bottom.

Boreholes 1, 2 and 3 in the pillar are 50 m deep, boreholes 4 and 5 above the drifts are 45 m deep. For temperature compensation of the measurements and for monitoring the temperature field at both ends of the monitoring stations resistance thermometers were installed.

Cementation of the stations in the boreholes was carried out using two different methods. Boreholes 1 and 2 were filled with an expanding saltcrete. Its expansion capacity was, according to manufacturer specification, about 0.3 to 0.5 vol.%. By expansion of the saltcrete, development of a close contact of the sensors with the salt rock should be accelerated. Thus, the primary stress state and stress changes could be measured early.

The second procedure consisted in backfilling of boreholes 3, 4 and 5 with a magnesite-salt-grout without expansion capacity. In order to get a close contact of sensors and salt rock, synthetic resin was injected into these boreholes. The borehole filling was forced open and the resulting cracks were filled with resin via perforated pipes. The injection pressure of 150 bar was hold till the resin was hardened. The stresses will be reduced significantly by shrinking of the resin and by volume reduction due to reaction heat decrease (see figures 3.1-15 and 3.1-16).

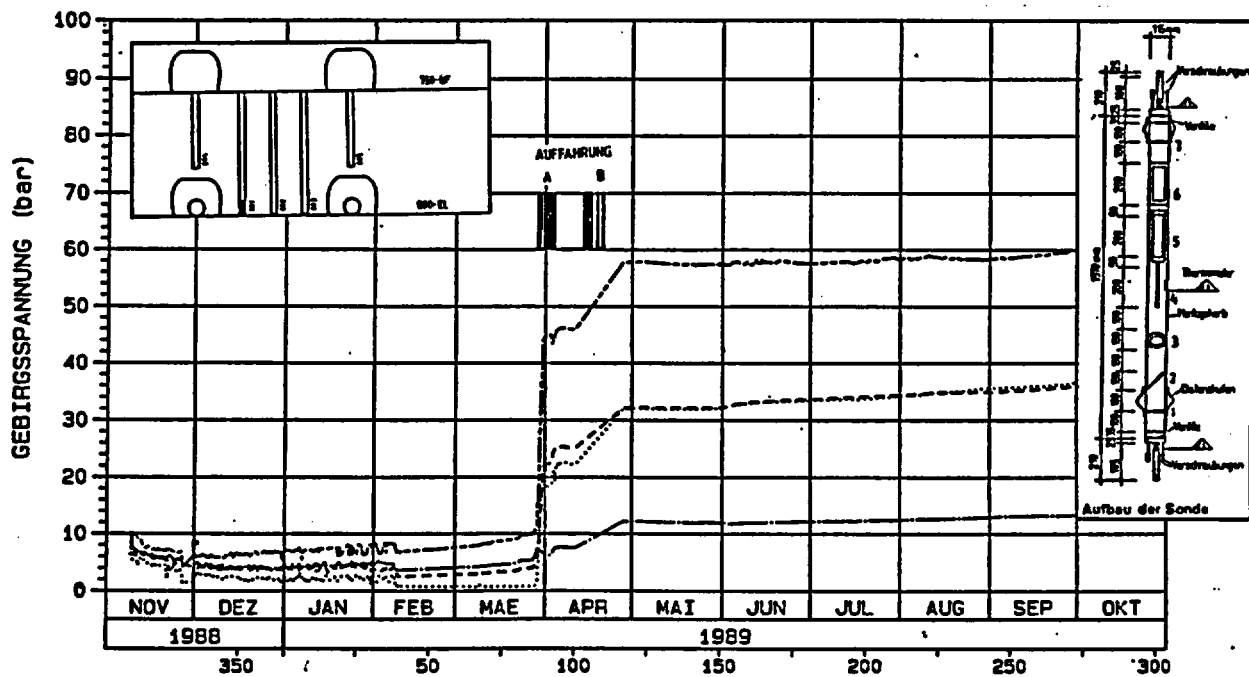
Also in boreholes 1 and 2 an additional injection was tried. However, that was not successful, presumably because the injection pipes were plugged. A pressure build-up was not observed.



KURVE	MST GEBER	MG	Teufe (m)	Richtung	HÖHE (m NN)	MESSEZEITRAUM VON / BIS	KOMPENSAT
-----	200 AFF 2	0	0	0	0	290389-210489	M200
.....	092 US004-1	S004	-44.405	vertikal	-597.405	091188-021089	OHNE
-----	093 US004-2	S004	-44.255	subh. läng	-597.255	091188-021089	OHNE
-----	094 US004-3	S004	-44.055	subh. quer	-597.055	091188-021089	OHNE
-----	095 US004-4	S004	-43.805	hor. längs	-596.805	091188-021089	OHNE

GEBIRGSSPANNUNG	
P A E - T S S	ANLAGE: S-Of 4/1
GESELLSCHAFT F. STRAHLEN- U. UMWELTFORSCHUNG (GSF)	DATUM: 30.10.89
Theodor-Heuss-Strasse 4	
3300 BRAUNSCHWEIG	

Fig. 3.1-15: Rock stresses measured in borehole 1

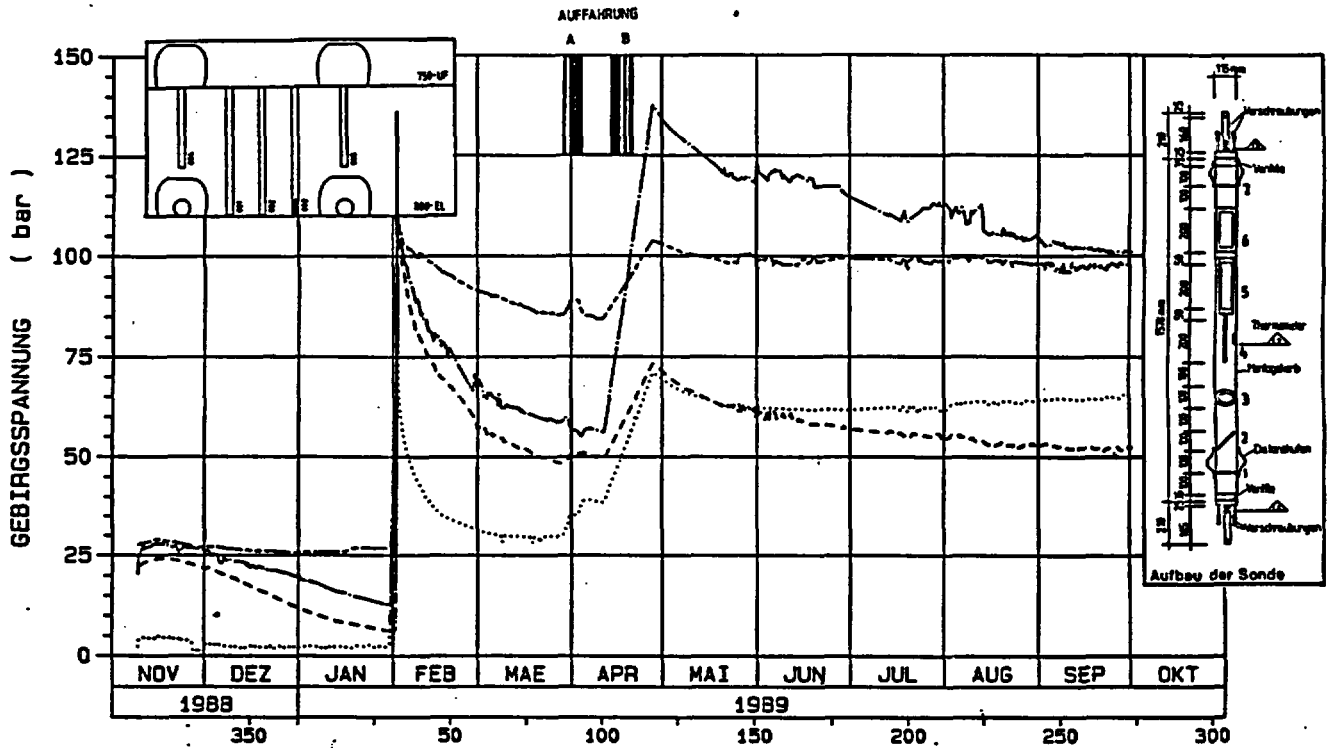


KURVE	MST GEBER	MG	Teufe (m)	Richtung	HÖHE (m NN)	MESSEZEITRAUM VON / BIS	KOMPENSAT
-----	200 AFF 2	0	0	0	0	290389-210489	M200
.....	071 US001-1	S001	-49.655	vertikal	-602.655	091188-021089	OHNE
-----	072 US001-2	S001	-49.505	subh. läng	-602.505	091188-021089	OHNE
-----	073 US001-3	S001	-49.305	subh. quer	-602.305	091188-021089	OHNE
-----	074 US001-4	S001	-49.055	hor. längs	-602.055	091188-021089	OHNE

GEBIRGSSPANNUNGEN	
P A E - T S S	ANLAGE: S-Of 1/1
GESELLSCHAFT F. STRAHLEN- U. UMWELTFORSCHUNG (GSF)	DATUM: 30.10.89
Theodor-Heuss-Strasse 4	
3300 BRAUNSCHWEIG	

Fig. 3.1-16: Rock stresses measured in borehole 3

Rock stresses measured in boreholes 1, 3 and 4 can be seen in figures 3.1-15 to 3.1-17. Excavation of the test drifts, shown in the diagrams by solid lines, caused significant stress changes. In boreholes 4 and 5 above the test drifts vertical stresses dropped to almost "0". Vertical stresses in the pillar (boreholes 1, 2 and 3) increased considerably.



KURVE	MST GERÄT	NO	Tiefe (m)	Richtung	HÖHE (m NN)	MESSZEITRAUM VON / BIS	KOMPENSAT
—————	200 AFF 2	0	0	0	0	290389-210489	M200
.....	085 US003-1	S003	-49.655	vertikal	-602.655	091188-021089	OHNE
-----	086 US003-2	S003	-49.505	subh. läng	-602.505	091188-021089	OHNE
-----	087 US003-3	S003	-49.305	subh. quer	-602.305	091188-021089	OHNE
-----	088 US003-4	S003	-49.055	hor. längs	-602.055	091188-021089	OHNE

GEBIRGSSPANNUNG	
P A E - T S S	ANLAGE: S-Of 3/1
GESELLSCHAFT F. STRAHLEN- U. UMWELTFORSCHUNG (GSF)	DATUM: 30.10.89
Theodor-Haus-Strasse 4 3300 BRAUNSCHWEIG	

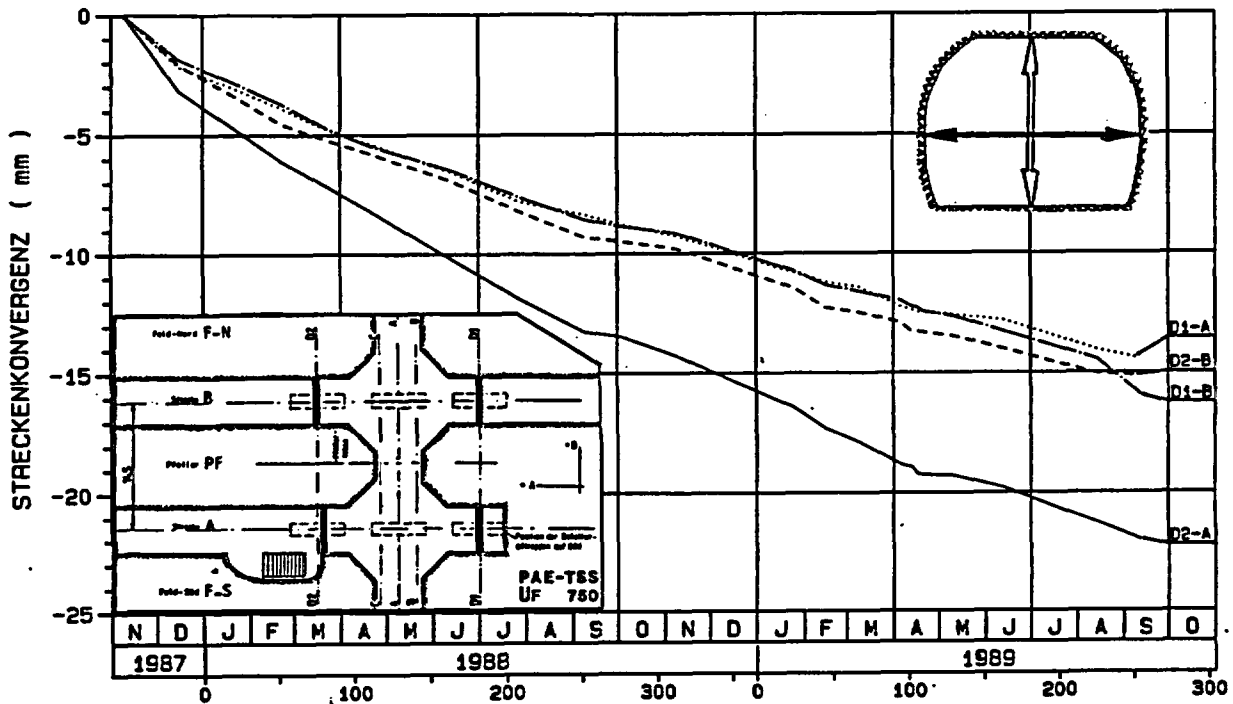
Fig. 3.1-17: Rock stresses measured in borehole 4

Horizontal stresses perpendicular to the test drifts increased above the drifts and decreased in the pillar. In boreholes 1 and 2 a different reaction was observed because in these boreholes no synthetic resin could be injected and the stress level was low. In these two boreholes horizontal stress increased to about 25 bar, the same value as in borehole 3.

At present the absolute quantity of the stresses cannot be assessed definitely because the development of the contact between rock salt and sensors was not finished.

Convergence measurement

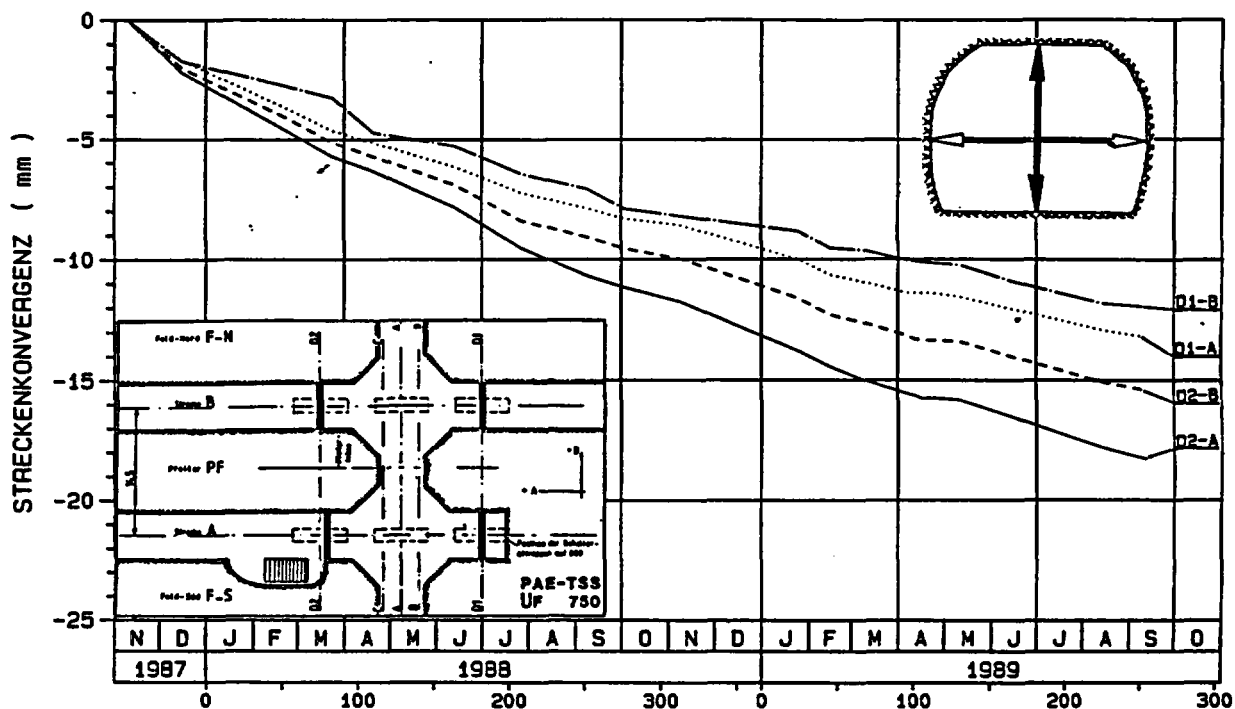
Convergence measurements are carried out since November 1987 in four sections in the overpass drifts (fig. 3.1-18 and 3.1-19). By these measurements the deformation behaviour of the rock in that specific mine region can be assessed. The shape of the curves in figures 3.1-18 and 3.1-19 is approximately linear, the average convergence rate being about 2‰ per year. Horizontal convergences in three sections are 1.6‰. In section D2 in drift A, adjacent to the measuring alcove, the horizontal convergence is 2.4‰ per year. Vertical convergences range between 1.6‰ and 2.5‰ per year. The greatest convergence rate was measured adjacent to the alcove.



KURVE	MST BEBER	NG	TEUFE (m)	RICHTUNG	HÖHE (m NN)	MESSZEITRAUM VON / BIS	KOMPENSAT
001	UK-A/D2V	D2-A	+2.00	HORIZONTAL	-553	091187-120989	OHNE
003	UK-A/D1H	D1-A	+2.00	HORIZONTAL	-553	091187-120989	OHNE
005	UK-B/D2H	D2-B	+2.00	HORIZONTAL	-553	091187-120989	OHNE
007	UK-B/D1H	D1-B	+2.00	HORIZONTAL	-553	091187-120989	OHNE

STRECKENKONVERGENZ	
PAE - KVG	ANLAGE: KVG-Of-t
GESELLSCHAFT F. STRAHLEN- U. UMWELTFORSCHUNG (GSF)	DATUM: 23.10.89
Theodor-Hauss-Strasse 4 3300 BRAUNSCHWEIG	

Fig. 3.1-18: Horizontal convergence in the overpass drifts



KURVE	MST GEBER	MQ	TEUFE (m)	RICHTUNG	HÖHE (m NN)	MESSZEITRAUM VON / BIS	KOMPENSAT
—	002 UK-A/D2V	D2-A	0 - 4.0	VERTIKAL	-553	091187-120989	OHNE
.....	004 UK-A/D1V	D1-A	0 - 4.0	VERTIKAL	-553	091187-120989	OHNE
- - -	008 UK-B/D2V	D2-B	0 - 4.0	VERTIKAL	-553	091187-120989	OHNE
- · - · -	008 UK-B/D1V	D1-B	0 - 4.0	VERTIKAL	-553	091187-120989	OHNE

STRECKENKONVERGENZ	
PAE - KV8	ANLAGE: KV8-ÖF-v
GESELLSCHAFT F. STRAHLEN- U. UMWELTFORSCHUNG (GSF)	DATUM: 23.10.89
Theodor-Heuss-Strasse 4 3300 BRAUNSCHWEIG	

Fig. 3.1-19: Vertical convergence in the overpass drifts

Test drift excavation on the 800-m-level in March and April 1989 caused in all the measuring sections a temporary retardation of the convergences which lasted till June 1989.

b) Studies from the test drifts at the 800-m-level

At the 800-m-level geotechnical instruments will be installed in boreholes drilled from the test drifts, in the backfill, and on the heater casks. Test drift excavation was conducted in March and April 1989. Subsequently boreholes and slots required for cables and pipes were mined.

Installation of instruments was commenced. Three convergence measuring sections for preliminary hand measurements were installed in sections A, E1, and E2 (figure 3.1-20). Measurements carried out so far show convergences considerably greater than those in the overpass drifts. Convergences mea-

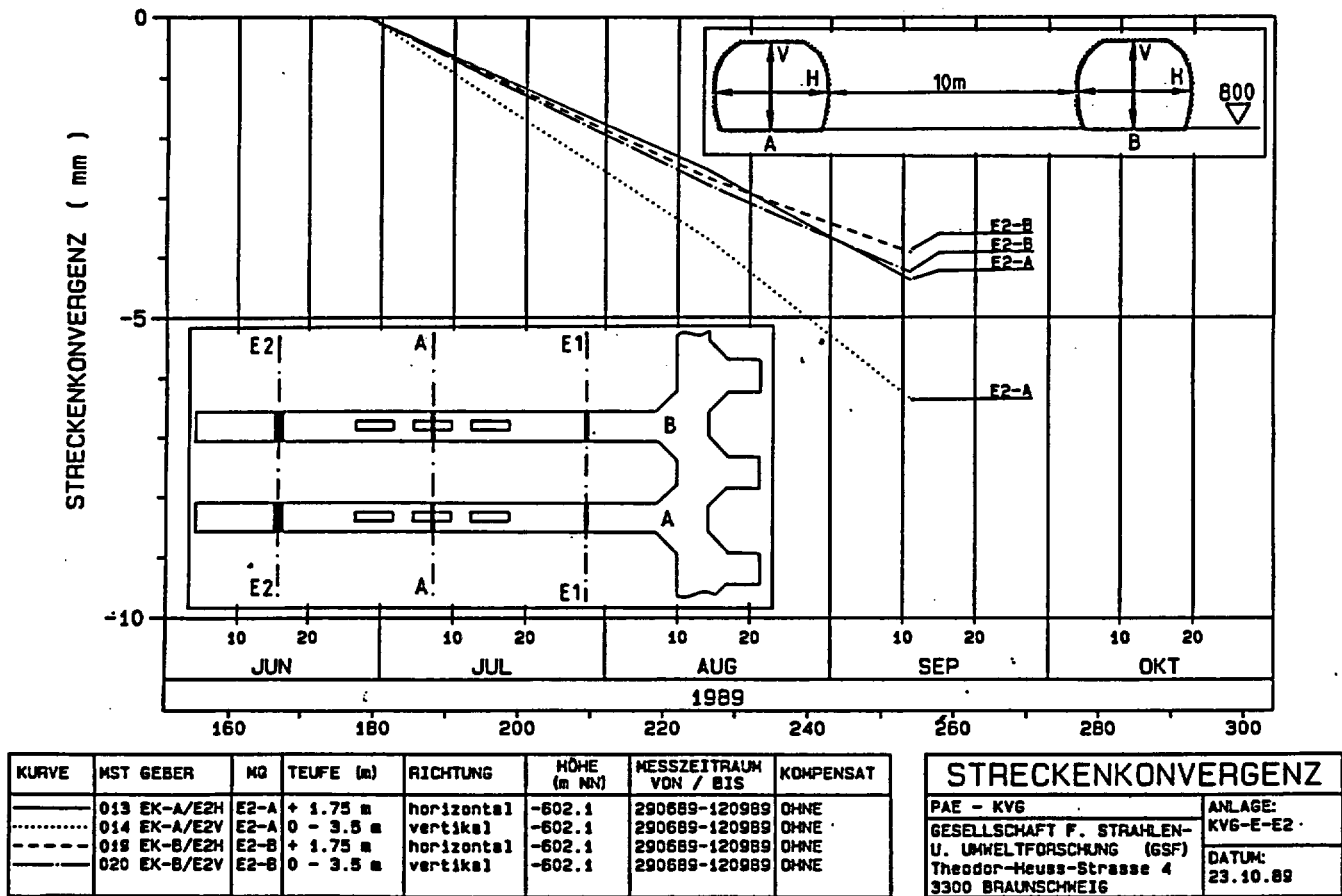


Fig. 3.1-20: Convergences in the test drifts (section E2)

sured in different sections differ significantly. Values extrapolated to annual convergence rates are summarized in table 3.1-1.

section	horizontal	vertikal
A	3,9	5,0
E1	2,7	4,3
E2-A		8,9
E2-B	4,4	5,7

Table 3.1-1: Average annual convergence rates in the test drifts (‰)

3.1.3 Future Work

Instrumentation of measuring boreholes and test drifts will be completed. Subsequently the rear ends of the test drifts will be backfilled. Heater canister installation and backfilling of the central and front sections will be carried out successively. During backfill emplacement the accompanying investigation program will be performed.

Investigations for assessment of the initial state of the salt rock will be continued.

3.2 Handling Tests for Drift Emplacement (HHV)

3.2.1 Objectives and Schedule

This project is carried out to establish the qualifications for approval and application of the 65 t POLLUX casks in time for the licensing procedure of the underground repository for heat-generating radioactive materials. The technical components for underground transport and for emplacement of the POLLUX casks must be designed and their approval by the mining authorities must be sought. For this purpose, reliable and safe handling under conditions relevant to a repository must be demonstrated by means of a non-radioactive large container of the original dimensions and weight. The responsibility for the development of the component parts and the execution of the tests is with DBE.

So far, the following milestones have been set for the implementation of Project Phase III, "Above-ground Tests," for the period Jan. 1, 1990 to Oct. 31, 1993:

- | | |
|---|------------|
| - Completion of planning work | 1990 |
| - Construction of the emplacement device | 1990/1991 |
| - Preparation of the test site above ground | 1991/1992 |
| - Test of the components above ground | 1992 |
| - Analysis of above-ground tests | 1992/1993. |

For the implementation of Project Phase IV, "Underground Tests," in 1992-1995, the following milestones have been proposed:

- | | |
|--|------------|
| - Preparation of the underground test site | 1992/1993 |
| - Underground testing of the components | 1993/1994 |
| - Analysis of the whole project | 1994/1995. |

3.2.2 Ongoing Work

Production planning for the "Transport Car for POLLUX Casks" has been completed and construction work has commenced. The non-radioactive large

container has been made as a dummy for prototype testing and is ready at the Landesbergen test site for use during the "Simulation of Shaft Hoisting" demonstration. The "Emplacement Device" specification has been approved for tendering on the basis of the results of a pre-examination by the Hannover Technical Inspectorate (TÜV).

3.2.3 Future Work

In the coming six months, production of the "Transport Car for POLLUX Casks" will be completed and final inspection will take place.

The transport car will be delivered to the Landesbergen test site for use with the non-radioactive large container in the "Simulation of Shaft Hoisting" demonstration. Invitations for tenders for planning and production of the emplacement device will be issued. In addition, an auxiliary bogey for the transport car will be designed for use in the tests in order to eliminate problems in operation.

3.3 Simulation of Shaft Hoisting (SST)

3.3.1 Objectives and Schedule

All important engineering and mining components and facilities for hoisting payloads of approx. 85 t must be proved to correspond to the state of the art. Where this cannot be proved by comparing with existing hoisting equipment, components and installations must be built and tested to show reliable and safe functioning in demonstrations under realistic conditions; this includes interlocking systems to prevent heavy loads from crashing into the shaft. Planning, implementing and analyzing of this project are responsibilities of DBE.

On the basis of the present tentative schedule, the following milestones have been earmarked for project implementation:

- | | |
|-----------------------------------|------------|
| - Construction of test rig | 1990/1991 |
| - Test execution | 1991 |
| - Execution of rope loading tests | 1990/1991 |
| - Analysis and general review | 1991/1992. |

3.3.2 Ongoing Work

3.3.2.1 Planning the Test Rig

In the period under review, the plans for completing the test rig and the engineering components, inclusive of stress analyses and the tendering documents for construction and commissioning of the test rig, will be completed. The bid will be submitted in January 1990.

3.3.2.2 Engineered Safety Studies

All important systems of the charging installation, the loaded transport car included, were investigated on the basis of the failure mode and effect analysis described in DIN 25, 448 to determine possible malfunctions with radio-

logical consequences to the operating personnel and effects on the entire installation.

The procedure is to identify relevant information about possible malfunctions and ways to overcome them. Failure of certain components, not a combination of component failures is assumed.

As an additional consequence of such an analysis it may become necessary to adopt further protective measures or change the design. In detecting possible malfunctions, those components of the charging equipment will be investigated which are defined below as being significant for radiation protection and safety under the restricted space conditions prevailing. Specifically, these are the transport car loaded with a POLLUX cask and

- the rail connection (cage bottom support and separate hinged rail),
- the vehicle lock in the intermediate bottom of the cage, and
- the charging unit.

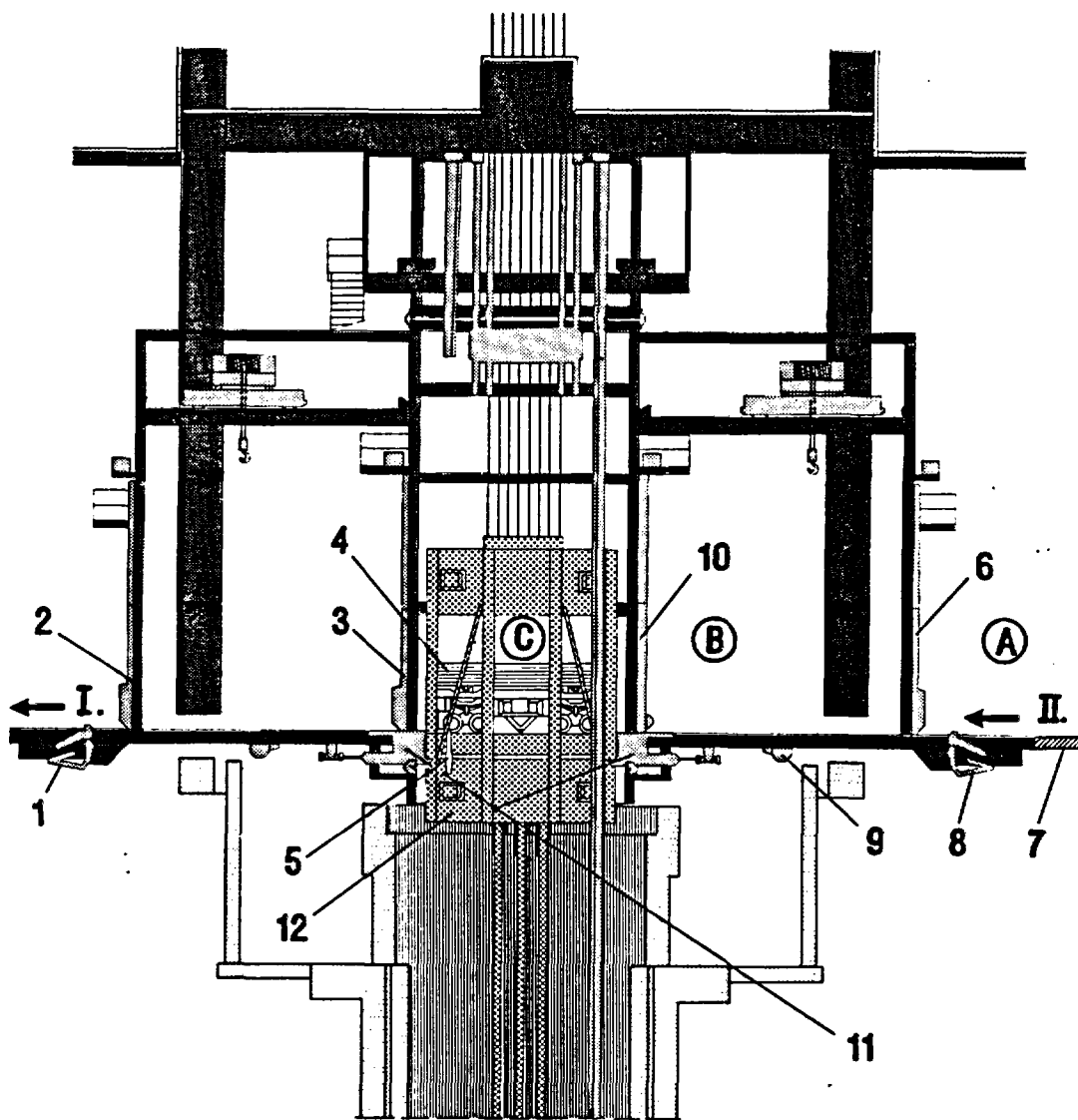
The arrangement of the components in the area of the charging unit above ground and the shaft station at the emplacement level is illustrated schematically in Figures 3.3-1 and 3.3-2.

The transport car has been investigated only in the condition in which it is loaded with a POLLUX cask, as the failure modes and the elimination of any operating problems will be more difficult under these circumstances than in an empty transport car. As the cage bottom support is monitored by the safety circuit of the shaft charging equipment and the lock gate is interlocked mechanically in with the intermediate cage bottom in the shaft, the transport car cannot be rushed onto the intermediate cage bottom when the supports are not engaged; this feature therefore has not been considered within the scope of the present work.

The following other aspects were also disregarded:

- Incorrect positioning of the transport car in the cage, as this is impossible by virtue of the design of the charging unit. The restraining sys-

- Ⓐ position of the transport car in front of the shaft lock (weigh-bridge)
 Ⓑ position of the transport car in the air lock
 Ⓒ position of the transport car in the cage



1. shaft lock 1
2. outer air lock gate 1
3. inner air lock gate 1
4. transport car loaded with POLLUX-cask
5. transport car arrestor
6. outer air lock gate 2
7. weigh-bridge

8. shaft lock 2
9. charging unit 2
10. inner air lock gate 2
11. intermediate cage bottom support combined with rail connection
12. hoisting cage

- I. decharging direction
 II. charging direction

Fig. 3.3-1: Arrangement of components and location of the transport car in the area of the above ground charging installation (source: SIEMAG 1988)

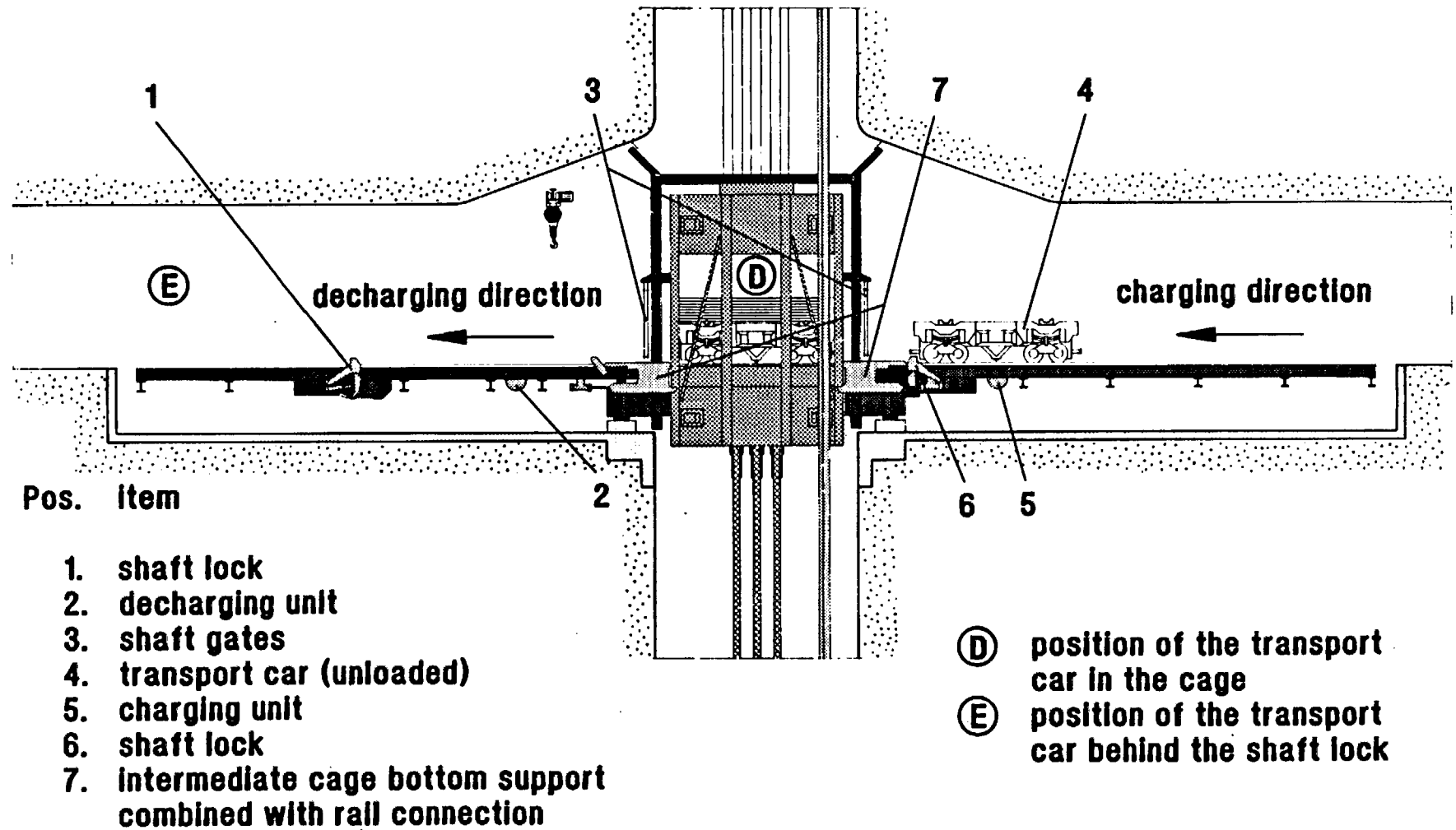


Fig. 3.3-2: Arrangement of components and location of the transport car in the area of the shaft station on the emplacement level (source: SIEMAG 1988)

tems (car lock, parking brake) ensure a correct transport car position both during hoisting and during set-down.

- Uneven lifting of the cage as a result of uneven loading of the ropes; the control system of the hoisting rope is designed in accordance with TAS in such a way that this is not possible.
- Blocking of two roller guides on one side of the cage with skewing of the cage; as the steel guides start to engage when there is a skew of approximately 2 cm, this prevents further dislocation into a skewed position.

The charging unit was investigated only with regard to its movement in conjunction with the loaded transport car. Movements without transport car were not taken into consideration, as malfunctions in operation can be remedied without radiological consequences.

The shaft lock and the inner air lock gate were not investigated, as they are designed to withstand an impact of the loaded transport car with a total mass of 85 t at a speed of 0.5 m/s.

For the purposes of the analysis, the units were subdivided into components or component groups. Accordingly, the possible failure modes are the result of the function of the components.

Component failures were assessed in accordance with the following criteria:

- **Maintenance**
Such effects do not lead to systems failure.
- **Systems Failure**
- **Inadmissible Systems Condition**
This effect might lead to a systems condition in which technical safety regulations could be infringed.
- **Hazardous Conditions**
The inherent hazard potential of the system is released.

In the case of the transport car, the

- stationary position
- in motion

operating conditions and positions in the area of the above ground charging installation defined during operation

- in front of the shaft lock (position A in Figure 3.3-1),
- in the air lock (position B in Figure 3.3-1),
- in the cage (position C in Figure 3.3-1)

were taken into consideration as well as the shaft station at the emplacement level

- in the cage (position D in Figure 3.3-2)
- behind the shaft lock (position E in Figure 3.3-2).

Possible malfunctions with radiological consequences are summarized in Table 3.3-1. For the area of shaft charging installations, the most serious failure effect was assumed to be a crash of the POLLUX cask from the transport car.

Such a case might arise if there are defects or malfunctions in the hinged rail assembly due to the separate designs of the intermediate cage bottom support and the bridging system. This possible failure effect leads to the recommendation that rails should be used which represent an integral part of the intermediate cage bottom support. Failure mode analysis and comparison of the stresses induced by malfunctions, using the load assumption for type B(U) qualification, therefore do not give rise to the assumption that malfunctions in the area of the charging installations above and below ground will in any way affect the tightness of the containment of radioactive substances or the shielding of radiation. Consequently, failures in the area of the charging system do not lead to accidental failures; possible radioactive consequences are due to the increased exposure of the operating personnel while attempting to correct a breakdown. The maintenance cases listed in Table 3.3-1 do not lead to radiological consequences.

Failed Component	Item	Failure Mode	Possible Causes	Failure Effect on the Transport Car	Failure Assessment
Transport car - stationary	A,B,C, D,E	Defect	Material defect, fatigue	Serviceable Maintenance case:	Maintenance case Systems failure
Transport car - moving	A - B B - C D - E	Defect	Material defect, fatigue	Serviceable not serviceable Derailment	Maintenance case Systems failure Systems failure
Rail connection - platform truck moving	B - C D - E	Defect	Material defect, fatigue, control defects	Derailment POLLUX cask leaves transport car	Inadmissible systems failure
Charging unit - with the transport car moving	A - B B - C D - E	Defect	Material defect, fatigue, control defects	Not serviceable	Systems failure
Transport car lock	C - D	Defect	Material defect, fatigue, control defects	Serviceable	Systems failure

* pursuant to Figure 3.3-1; 3.3-2

Table 3.3-1: Results of the Failure Mode Analysis

3.3.2.3 Suitability of the Ropes for a Shaft Hoisting System with 85 t Payload

The concept of a shaft hoisting system with 85 t payload is based on two modes of operation:

- Haulage of 85 t payload at a hoisting speed of 5 m/s, and
- haulage of 30 t payload at a hoisting speed of 12 m/s.

The hoist is designed as a tower with a single-stranded cage hoisting system with counterweight. The hoisting ropes are 8 Warrington seal ropes with 51 mm nominal diameter and a fibre insert or three-ply flat ropes of 50 mm nominal diameter and with fibre inserts. Three underslung flat ropes of 252 mm x 36 mm or 264 mm x 38 mm are provided as a balancing weight.

The loading process differs from that employed in normal mine hoisting systems in that the payload is first pushed onto the fixed intermediate cage bottom without actually applying any load to the ropes. Then the cage is lifted slightly at a lower speed of 1 cm/s, at which point the ropes take the strain. The suitability of these ropes for a hoisting system of 85 t payload has been assessed by the rope test authority of the Westfälische Berggewerkschaftskasse (WBK) and rated as follows:

Both flat designs of the balance ropes are suitable for the loads envisaged and under the prevailing transport and climatic conditions.

The hoisting ropes take up the payload of 85 t over a rope run between a driving wheel and an intermediate linkage of 34.5 m, with a rise in tensile stress in the rope of approx. 30 N mm⁻²s⁻¹. This rise in tensile stress in the rope is four times the stress induced in the ropes of a conventional modern mine hoisting system (7.5 N mm⁻²s⁻¹).

For the proposed mode of operation, the three-ply flat ropes are more suitable than the circular section ropes, and there are no safety objections to their use. However, it is not possible to make reliable statements about a decrease in the load carrying capacity (= lifetime) of the ropes, as the planned speed during hoisting of the load of 1 cm/s makes the rate of loading so

much higher than the empirical information gained with conventional hoisting systems that reliable extrapolation does not appear feasible.

The fourfold increase in tensile stress in the planned installation is not caused in the stationary rope, but when the rope slowly moves over the wheel (as distinct from conventional hoisting systems). This means that part of the spatial movement of the wires in the rope on the wheel can take place without significant impediment to deformation and friction. Notwithstanding this fact, quantitative information about the life of the rope cannot be given without trials. During an earthquake, only vertical movements of the cage and rope supports are capable of generating additional tensile stresses in the wires of the cable. The maximum tensile stress here is produced during uniform displacement of the rope support or cage over the shortest possible distance between the driving wheel and the intermediate linkage, i.e., when the cage is close to the uppermost end stop. The resulting increase in stress is on the order of approx. 140 N/mm², i.e. clearly below the stress increase of 500 N/mm² regarded to be admissible with respect to safety in the event of an earthquake. Accordingly, a crash of the cage into the shaft needs not be anticipated. However, it is recommended that a rope be taken out of service after exposure to this kind of stress by an earthquake.

3.3.3 Future Work

Work in the next six months will be carried out on the basis of a revised project description and the tentative schedule. On this basis, the contract for construction of the test rig and for commencement of production planning is to be awarded. Experiments at the Tremonia test facility in Dortmund are being prepared in cooperation with Deutsche Montan Technologie (DMT) to investigate rope loading at the time of load application. The failure trees for assessing the reliability of the components fitted to the test rig will be updated in accordance with the implementation plan.

3.4 Active Handling Experiments with Neutron Sources (AHE)

3.4.1 Objectives and Schedule

Within the scope of the program for the direct disposal of spent fuel, the new active handling experiment with neutron sources has the objective of investigating the radiological problems underground caused by direct neutron radiation and neutron radiation scattered by the salt rock during the handling of POLLUX casks and transfer casks for canisters.

The radiologic investigations will be performed with the aid of a shielded Cf-252 neutron source which should make it possible to simulate the energy spectrum of neutron radiation emitted by a POLLUX cask and by a transfer cask carrying a spent fuel canister.

Investigations regarding the radiation exposure of the operating personnel will be performed in existing tunnels of the Asse salt mine of GSF.

At the present, the following milestones have been specified for the implementation in accordance with the revised experimental plan for the period until 30.09.1993.

- | | |
|--|-----------|
| - Implementation of planning work and permission procedure | 1990/1991 |
| - Construction and procurement of equipment and components | 1991/1992 |
| - Performance of tests | 1992/1993 |
| - Analysis of tests | 1993. |

3.4.2 Ongoing Work

3.4.2.1 Calculations Comparing the Fraction of Scattered Radiation in a Neutron Dose Measurement at a Shielding Capsule with that at a POLLUX Cask in a Drift in Saline Rock

On behalf of KfK/PAE, H.G. Vogt calculated the ratio of the neutron dose rates, with and without scattered radiation, to the solid saline rock at a (small) shielding capsule and a POLLUX cask, both emplaced in a drift in a repository mine /3-5/.

The calculations were designed to furnish information about the transferability of measurements of the scattered radiation fraction in the neutron dose rate performed with a shielding capsule, as planned for the active handling experiment with neutron sources, to the real conditions existing in the repository storage of POLLUX casks, and to provide some indications as to a suitable design of a shielding capsule, respectively.

Two drift geometries were assumed as a basis for the calculations:

- Emplacement drift (fig. 3.4-1),
- main drift (fig. 3.4-2).

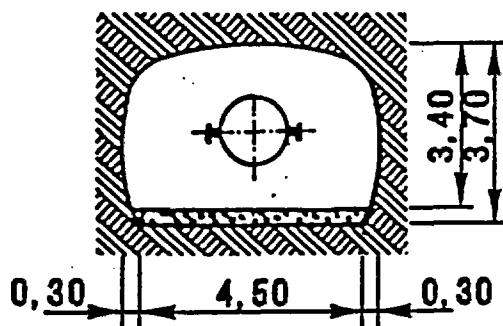


Fig. 3.4-1: Drift cross section of geometry 1; dimensions in m

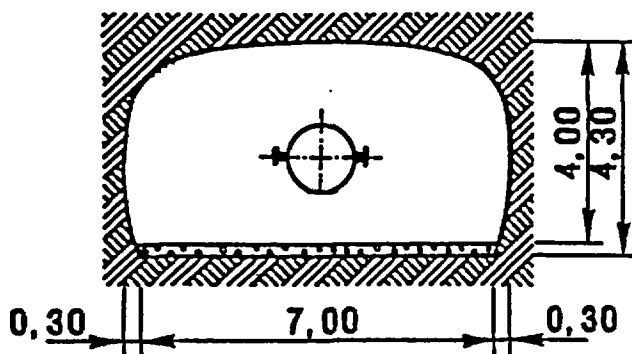


Fig. 3.4-2: Drift cross section of geometry 2; dimensions in m

Also, three container configurations were assumed:

- POLLUX container (fig. 3.4-4),
- shielding capsule (fig. 3.4-5 and fig. 3.4-3),
- shielding capsule arranged in a steel cylinder (fig. 3.4-6).

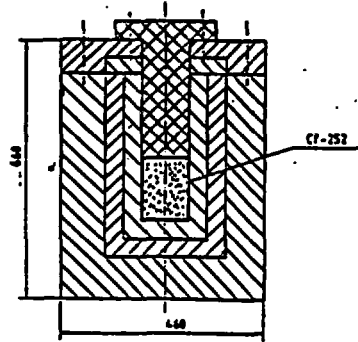


Fig. 3.4-3: Section through the shielding capsule; dimensions in m

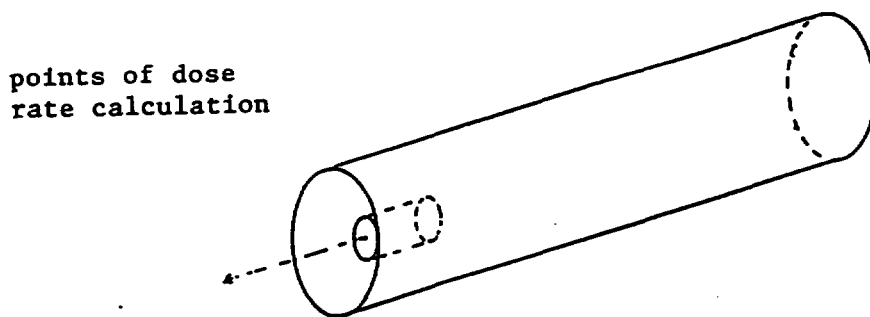


Fig. 3.4-4: Geometry of the POLLUX cask

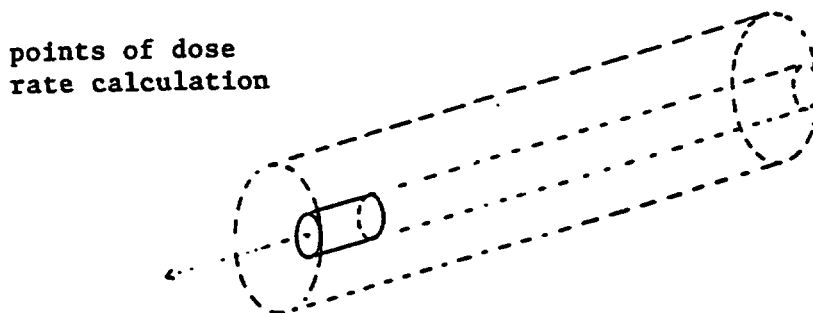


Fig. 3.4-5: Geometry of the shielding capsule

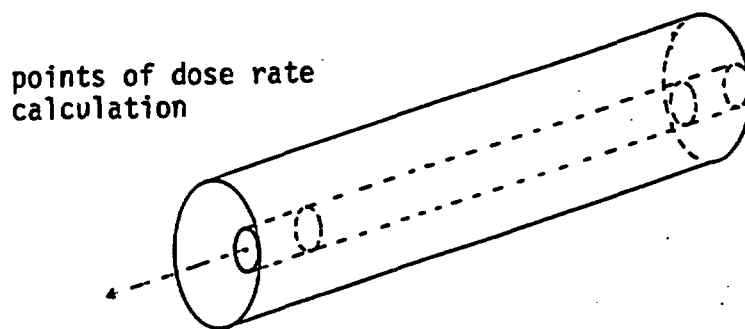


Fig. 3.4-6: Geometry of the shielding capsule in the steel cylinder

The latter configuration was to be used to study to what extent a steel cylinder of the external dimensions of the POLLUX cask, in which the shielding cask is installed, can be employed to detect secondary scattering effects, i.e., to what extent test conditions with a shielding capsule can be better adapted to real conditions with the POLLUX cask.

In the scattered radiation calculations performed, the surfaces of the shielding capsule and of the POLLUX cask were assumed as neutron sources. The shielding capsule is taken to be a solid steel cylinder 460 mm in diameter and 660 mm high. The POLLUX cask, and the steel cylinder acting as a scatterer, are assumed to have the same dimensions of 1,542 mm diameter and 5,462 mm length. The POLLUX cask is given as a solid made of steel. The steel cylinder of 5 cm thickness, which is open at the end faces, is cut open along its surface to allow the shielding capsule to be inserted in this position, thus simulating a section of the source surface of the POLLUX cask.

The sources are positioned in such a way that the longitudinal axes of the source casks extend parallel to the axis of the drift and, corresponding to the transport position, the POLLUX cask and the steel cylinder are 100 cm from the floor. The longitudinal axes of the casks are located at half the width of the drift cross section. The shielding capsule is laterally offset from the center of the drift, which corresponds to its position in the steel cylinder. This also applies to the calculations for the shielding capsule without the steel cylinder. The shielding capsule is arranged at eight positions over the entire length of the steel cylinder.

The surface points are located in extensions of the longitudinal axis of the shielding capsule at various distances from the end faces. These surface points are assumed also for the case of the POLLUX cask.

A special version of the SAM-CE Monte Carlo program, which simulates radiation transport, is used for the calculations /3-6/.

The calculations of scattered radiation are based on the given source data for the shielding capsule and the POLLUX cask. The barrel and end faces of these two containers were assumed to be neutron source areas. To determine the energy spectrum of the source neutrons, the results of one-dimensional transport calculations for the shielding capsule with a Cf-252 source were used as indicated in fig. 3.4-3 /3-7/. The energy dependent neutron flux densities on the barrel surface resulting from these calculations were normalized and set up as the neutron spectrum at all surface points both of the shielding capsule and the POLLUX cask. A cosine distribution was assumed as the angular distribution of the source neutrons.

The calculations were run for the two drift cross sections and the three container configurations for eight surface points at distances between 1 m and 20 m from the end faces of the containers. For the case of the shielding capsule with the steel cylinder, a total of eight different positions of the shielding capsule along the steel cylinder were investigated. The ratios of the equivalent dose rates, H_s with the saline environment and H_0 without the saline environment, provided the relative fractions of scattered radiation for the geometries examined.

The most important findings are plotted in figs. 3.4-7 to 3.4-10.

Figures 3.4-7 and 3.4-8 indicate the absolute dose rates to be expected at distances of up to 20 m from the end face of the POLLUX cask and the shielding capsule, respectively. The results always refer to the total source strength of 1 photon/s at the surface of the containers. In accordance with the ratio of the surfaces of the POLLUX cask and the shielding capsule, the source density per unit area is roughly 23.5 times higher on the capsule surface than on the POLLUX cask. On the other hand, the end face of the POLLUX cask, which is decisive for the dose rate in the absence of the saline environment, is approx.

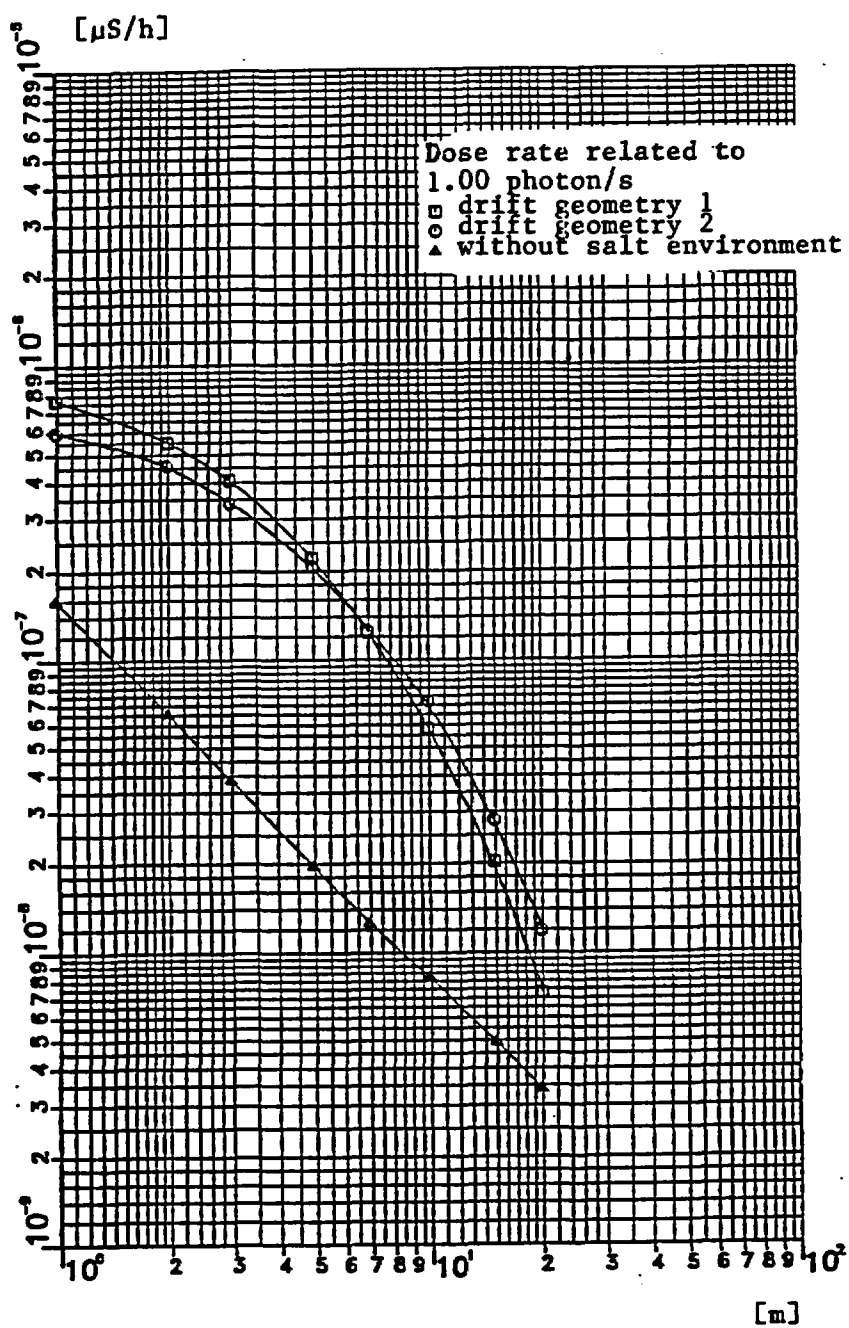


Fig. 3.4-7: Dose rate at the POLLUX cask plottet as a function of the distance from the container end face

11.2 times larger than that of the shielding capsule. Relative to the total source strength, the dose rate, H_s , for the configuration with the saline environment is a factor of 3 or 4 higher in the shielding capsule than in the POLLUX cask. The dose rates without the saline environment differ by approx. a factor of 10 for the two containers at 1 m distance.

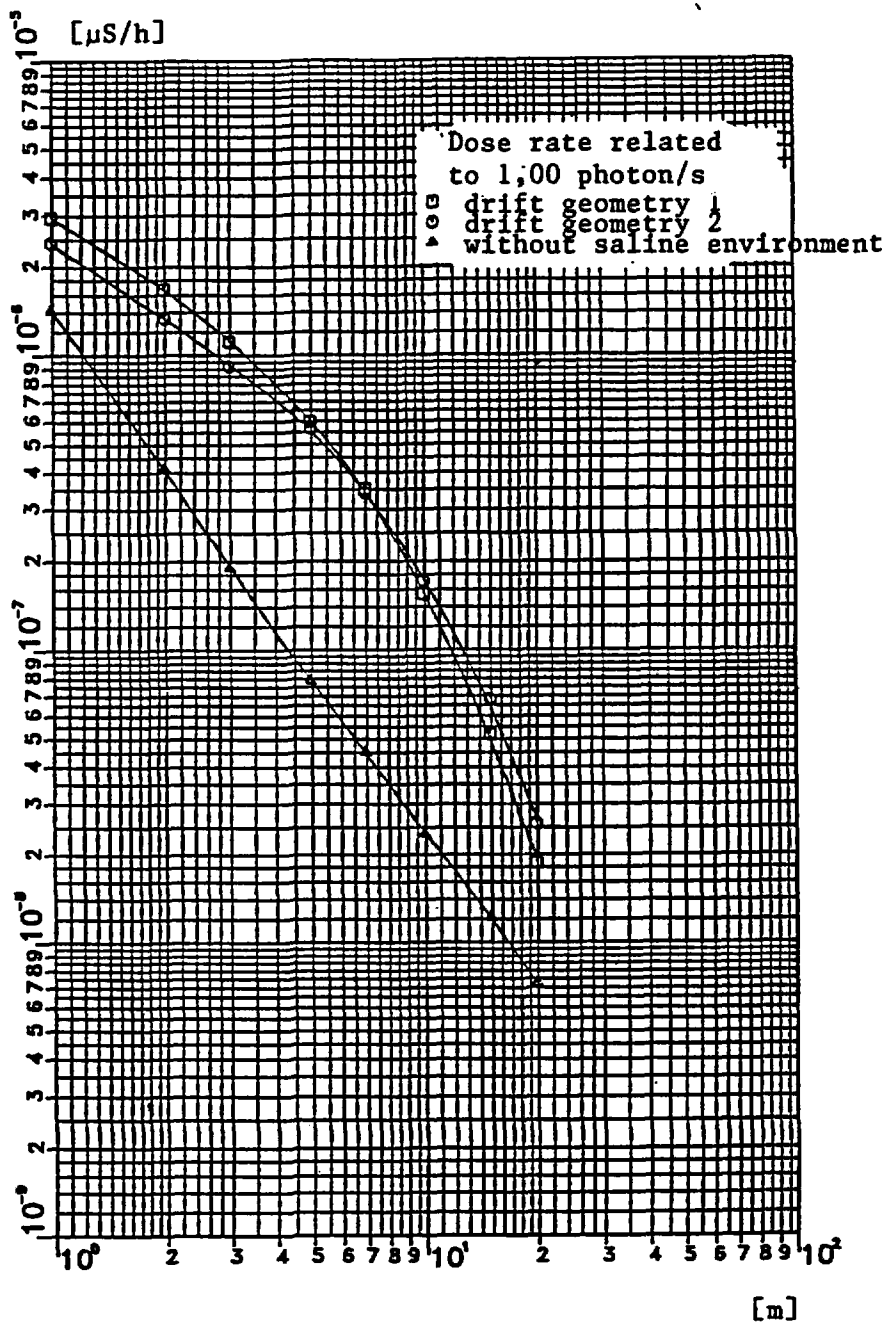


Fig. 3.4-8: Dose rate at the shielding cask plottet as a function of the distance from the container end face

Figures 3.4-9 and 3.4-10 show relative fractions of scattered radiation (relative to the dose rate in the absence of the saline environment) plottet as a function of the distance from the end faces of the containers. The curves shown in fig. 3.4-9 for the POLLUX cask and the shielding capsule clearly indicate that the fraction of scattered radiation for the shielding capsule at distances of up to 3 m from the container end faces is less than 60% of the fraci-

ton with the POLLUX cask, and will exceed that of the POLLUX container only at distances above 10 m. The curves for the two source geometries, POLLUX cask and shielding capsule, are relatively similar. However, in the case of the POLLUX cask, the maximum level is attained at approx. 5 m from the end face of the container, as compared to some 8 m for the shielding capsule.

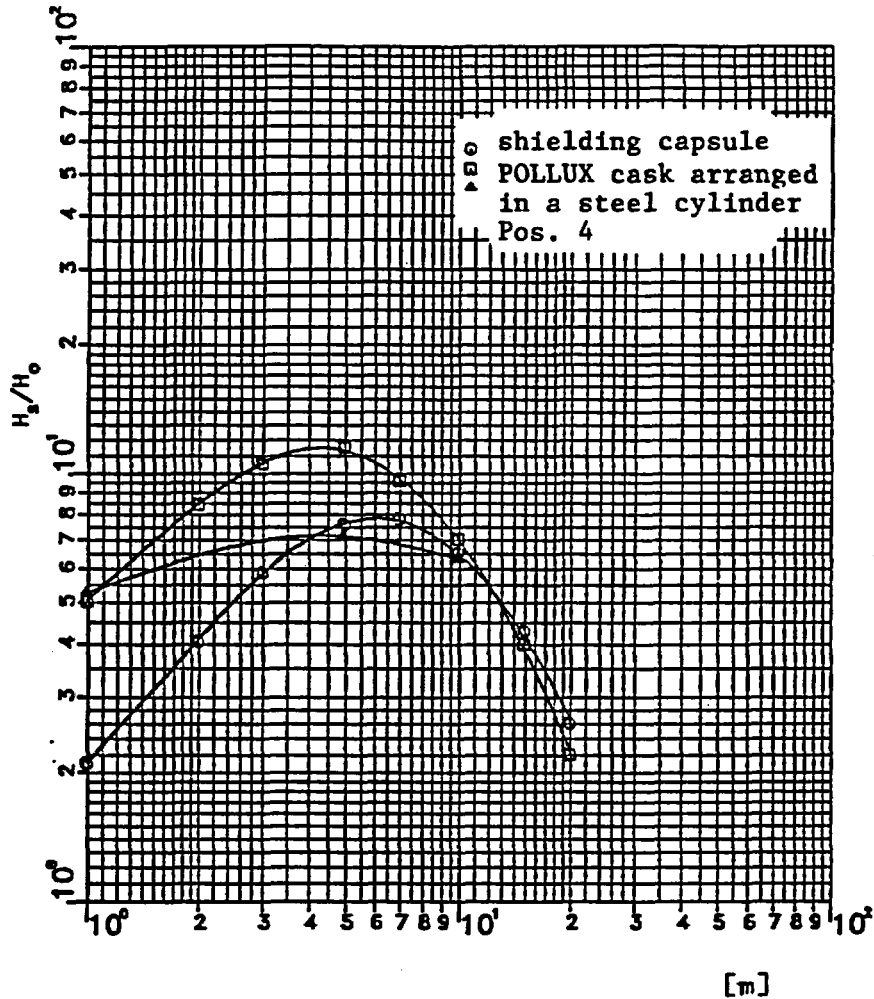


Fig. 3.4-9: Relative fractions of scattered radiation for POLLUX container and shielding capsule for drift geometry 1

The influence of the steel cylinder used to simulate the scattering surface of the POLLUX cask can be seen from fig. 3.4-9 and 3.4-10. The curve for the shielding capsule in the steel cylinder in fig. 3.4-9 is based on the source geometry as shown in fig. 3.4-6. Figure 3.4-10 indicates not only the relative fractions of scattered radiation for the POLLUX cask, but also the fractions of scattered radiation resulting if, for each surface point examined, the equivalent doses are summed up at all positions which may be taken up by the

shielding capsule along the steel cylinder, and are divided by the sum total of the corresponding doses obtained in the open air. The plots show that the steel cylinder does not improve the simulation of conditions at the POLLUX container.

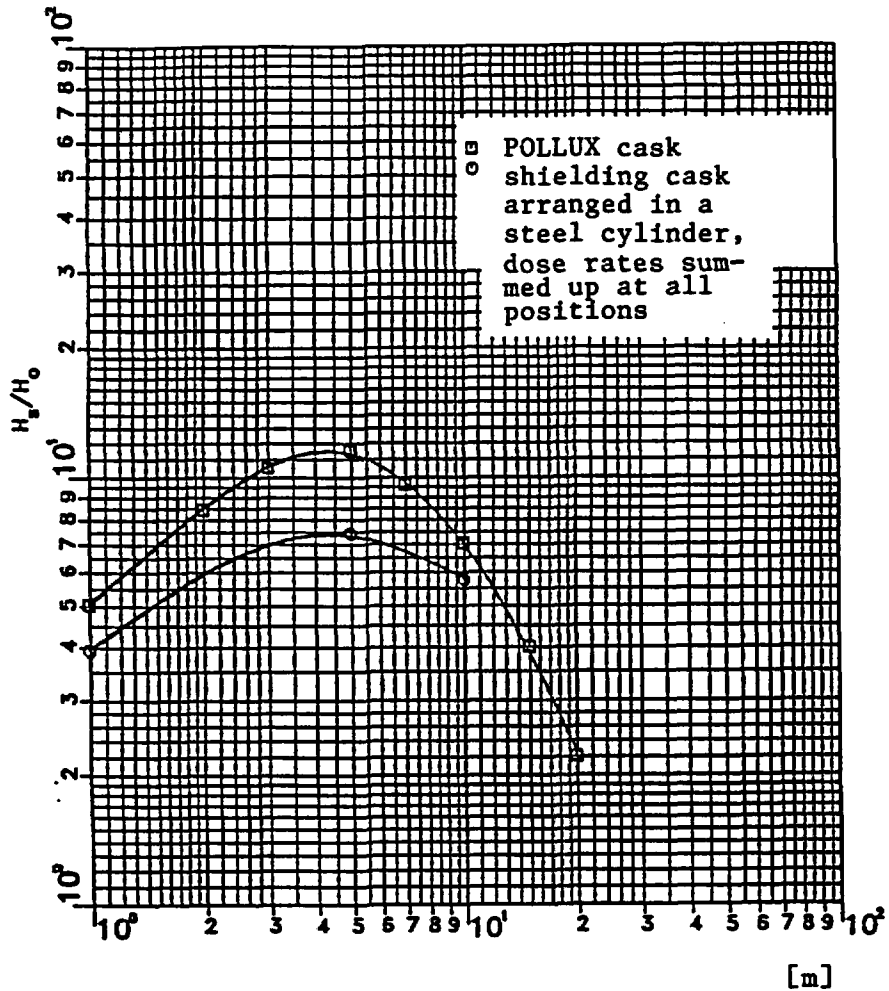


Fig. 3.4-10: Relative fractions of scattered radiation for POLLUX cask in the drift geometries 1 and 2

The comparison of the calculated results for the POLLUX cask and the shielding capsule indicates that results measured with the shielding capsule cannot simply be transferred to the case of the POLLUX cask. This is true at least in those cases in which the shielding capsule is designed as described here.

3.4.2.2 New Working Program

The revised working program for the AHE concentrates on the following points:

- Measurement of the neutron dose rate attributable to direct radiation and due to neutrons scattered by the salt rock
- Investigation of irregularities of shielding (gaps, passages for ropes)
- Verification of model calculations
- Determination of relevant data for the minimization of radiation exposure of the operating personnel.

The design of the shielded neutron source and the further development of theoretical codes has special significance, since it is essential that the experimental results are applicable to the use of transfer casks and POLLUX casks underground. The shielded radiation source for the production of neutron scatter in the tunnels of a salt mine is therefore characterised as follows.

- The filling with Cf-252 as the neutron source (s) and, where appropriate, with additional material must be designed in such a way that the spacial distribution of the radiation field and the neutron spectrum resembles a POLLUX cask and a transfer cask and so that the limit values for the dose rate (2 mSv/h at the surface, 0.1 mSv/h at a distance of 1 m) are not exceeded.
- The mechanical design has to meet the requirements for type A qualification in combination with the shielding container.

The experimental program provides for a reference measurement of the direct neutron radiation above ground without the effect of rock salt and closed rooms. Furthermore, the program provides measurements underground during which the effects of the geometry of tunnels and of the rock salt on the neutron scatter are to be investigated. In order to be able to derive quantitative information about the radiological exposure of the operating personnel in a repository, extensive doses rate measurements will take place

with directly emitted and scattered neutrons and then compared with calculations.

To simulate the irregularities of any shielding model tests will be designed to determine the dose rate at air gaps and through rope passages. The model tests will be performed using a shielded Cf-252 neutron source and the necessary measuring devices. This partial test can be performed for example in a workshop which has been designated a control zone.

3.4.3 Future Work

It is intended to perform one parameter study to determine the most favourable shielding capsule geometries which provide for optimum transferability of the dose rate calculation.

On the basis of this parameter study the design and shape of the shielded neutron sources for the trials for neutron back scatter underground in tunnels and for the model tests of shielding irregularities will be performed.

CONTENTS

4	<i>SYSTEMS ANALYSIS DUAL-PURPOSE REPOSITORY</i>	4-1
4.1	Systems Evaluation and Future Program	4-1
4.2	Parameter Variations	4-2
4.2.1	Parameter Variations	4-2
4.2.2	Variation of Initial Pressure	4-5

4 SYSTEMS ANALYSIS DUAL-PURPOSE REPOSITORY

4.1 Systems Evaluation and Future Program

The disposal concepts as designed between 1985 and 1989 were subject to an evaluation process /4-1/ which led to include concepts BD1 and D* - the latter being 3-level drift emplacement - in the future program. It was further agreed that the pure borehole emplacement concept should also be included so that an alternative were at hand if the shaft transport of the heavy POLLUX casks posed an insurmountable problem. In addition, areas were identified where the concept evaluation proved inadequate making evident future R&D needs. The advisory group which accompanies the systems analysis specified the future program which is subdivided in two parts, namely, site dependent and site independent studies. "Site dependent" is related to the model assumption concerning the Gorleben salt dome. The program is roughly structured as follows:

- 1 Boundary conditions, input data update
- 2 Site-independent repository studies
 - 2.1 Basic considerations concerning long-term safety
 - 2.2 Performance goals of technical barriers
 - 2.3 Evaluation of multi-level drift emplacement
 - 2.4 Impacts of high burnup and termination of recycling on repository design (direct disposal of MOX and reprocessed U)
 - 2.5 Impacts of a variation of the near-field design temperature (200°C)
 - 2.6 In-depth analysis of radiological safety
 - 2.7 Emplacement strategies
- 3 Site-dependent repository studies
 - 3.1 Conceptual design of emplacement panels for concepts BD1 and D*
 - 3.2 Utilization of existing computer codes
 - 3.3 Development of computer codes
 - 3.4 Repository safeguards
 - 3.5 Special safeguards needs.

4.2 Parameter Variations

Preliminary calculations pertaining to part 2.3 of the aforementioned program have been carried out. Former thermomechanical calculations for the access drift adjacent to a spent fuel emplacement panel were solely based upon a simplified model of rock salt behavior including thermoelastic and stationary (secondary) creep /4-1/. Laboratory tests with rock salt, however, exhibit both transient and stationary creep deformation. Neglecting of transient (primary) creep results in an underestimate of the room closure rates. It is well known that different zones within a given salt dome show different creep behavior due to changes in the mineralogical composition, grain size distribution, and water content. Therefore, in a first step, the sensitivity of calculations with respect to parameters governing the creep law have been investigated. Subsequently, calculations were performed to demonstrate the influence of the lithostatic pressure on the deformation within an access drift. These calculations provide first results related to room closure of the access drift in the case of concept D, three-level drift emplacement.

4.2.1 Parameter Variations

The following creep laws were used:

- a) BGR 1: It is characterized by a high creep capacity of rock salt /4-1, 4-2/.
- b) Benchmark: This corresponds to BGR 1 except for the constant A multiplied by 2 and Young's modulus divided by 2. The reduction of the elasticity was intended to model short-term effects immediately after excavation (e.g., plasticity and primary creep). This law proved successful in simulating in-situ tests within the benchmark project "COSA" /4-3/.
- c) BGR 2: It has been derived by BGR from measurements done with Gorleben salt samples /4-4/; it shows a modified temperature dependence and a low creep capacity of rock salt at room temperature.

These creep laws are compared in Fig. 4-1 and formulated in Table 4-1. Several calculations were performed in order to demonstrate the impact of creep laws upon the room closure in access drifts. The FE-grid, the boundary conditions, and the temperature history of the spent fuel emplacement panel were chosen as in /4-5/.

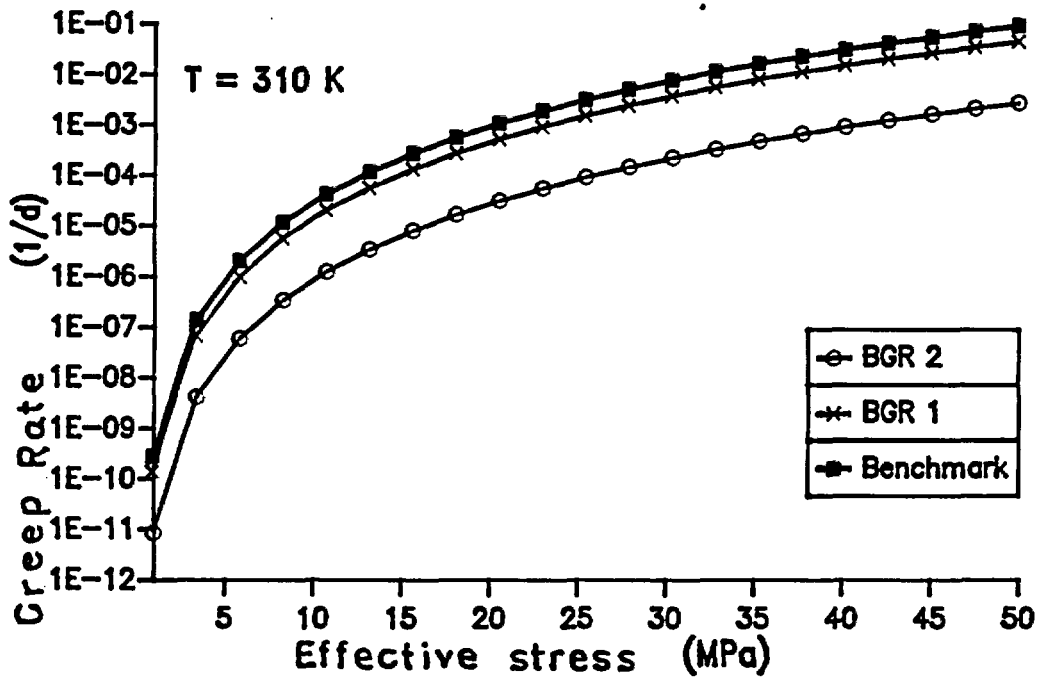


Fig. 4-1: Comparison of creep laws

Creep Law	A 1/d	Q kJ/mol	n -	E MPa	ν -
(BGR 1) $\dot{\epsilon}_c = A \sigma_{\text{eff}}^n \exp(-Q/RT)$	0.18	54.0	5	24,000	0.3
(benchmark) $\dot{\epsilon}_c = A \sigma_{\text{eff}}^n \exp(-Q/RT)$	0.36	54.0	5	12,000	0.3
(BGR 2) $\dot{\epsilon}_c = (A_1 \exp(-Q_1/RT) + A_2 \exp(-Q_2/RT)) \sigma_{\text{eff}}^n$	0.05	58.0	5	24,000	0.3
	2.1E6	113.0			

$\dot{\epsilon}_c$: stationary creep velocity (1/d)

σ_{eff} : effective stress (MPa)

T : temperature (K)

R = $8,314 \times 10^{-3}$ kJ/mol·K

Table 4-1: Creep laws and material parameters

Figure 4-2 shows horizontal and vertical displacements as a function of time, Fig. 4-3 gives the ensuing volume change. These results demonstrate a strong dependence upon the creep law. The results previously obtained with creep law BGR 1 /4-5/ are right between the two other alternatives. Room closure

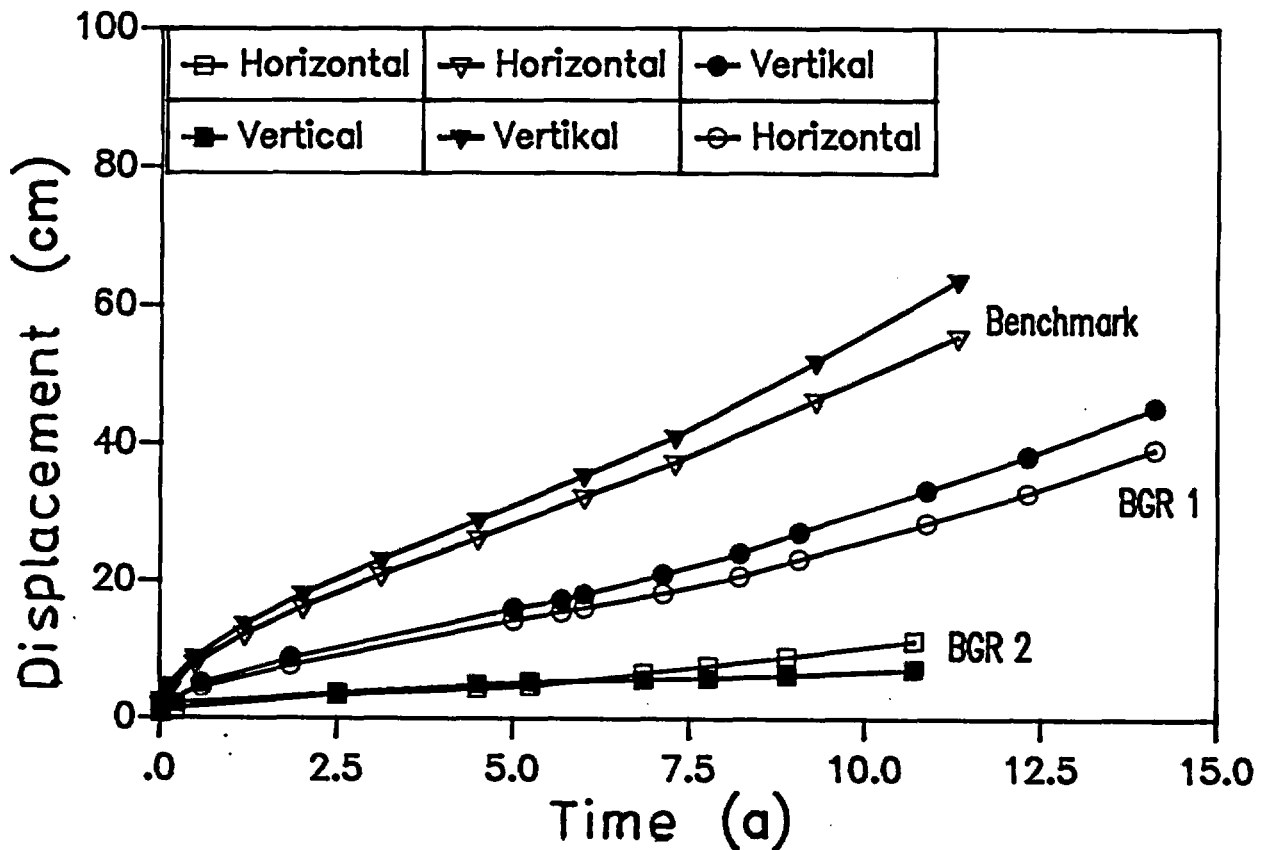


Fig. 4-2: Displacement in access drift adjacent to spent fuel emplacement panel

according to BGR 2 is much lower than in the other cases; it is also lower than the average values typical for open drifts in rock salt formations ($\sim 1\%/a$ at a depth of 800 m).

Defensible results for long periods of time can only be gained if material laws and parameters are well known. Supplementary parameter variations can be used to generate suitable results.

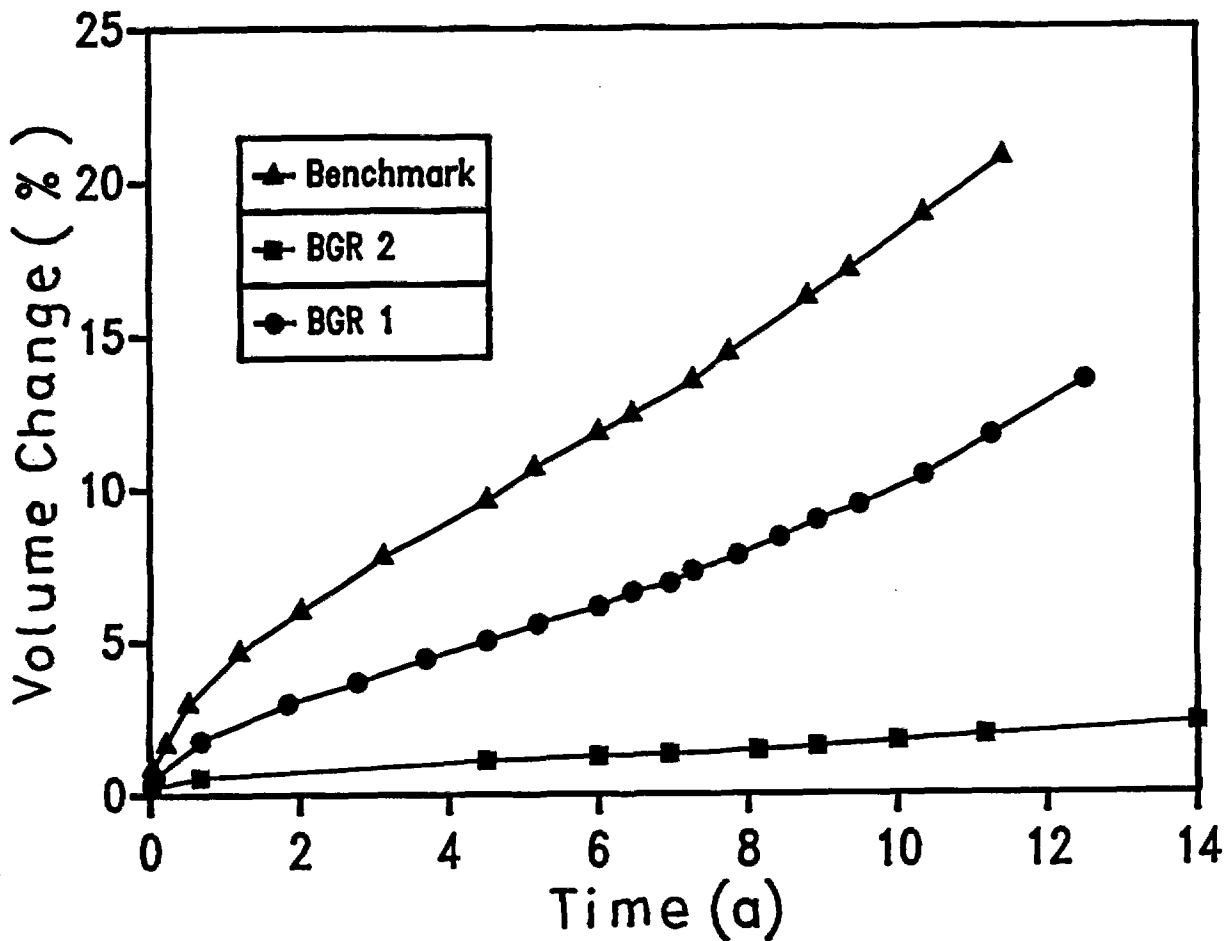


Fig. 4-3: Creep in access drift for three creep laws

4.2.2 Variation of Initial Pressure

These calculations aimed at assessing the impact of the emplacement depth on the room closure in access drifts. They were intended to give an idea about the situation in the case of three-level drift emplacement (concept D). The calculations were based on the same FE-model as already used within this R&D-program, whereby the lithostatic pressure was changed according to the emplacement depth lying between 870 and 1,170 m. This led to the following pressure boundary conditions:

- a) 18 MPa: reference case, emplacement horizon at 870 m
- b) 22 MPa: 1,020 m
- c) 25 MPa: 1,170 m.

For the cases b and c the calculations were restricted to a period of 7 years. Figure 4-4 shows the ensuing volume changes which, in the cases b and c, are twice as large during the cold phase ($t \leq 5$ yr). This is due to the strong stress dependence of the creep law.

To recapitulate, these results are only preliminary in nature and cannot be used directly to evaluate concept D, especially because the interference of the three levels has been omitted from modelling. Detailed calculations are planned for the future.

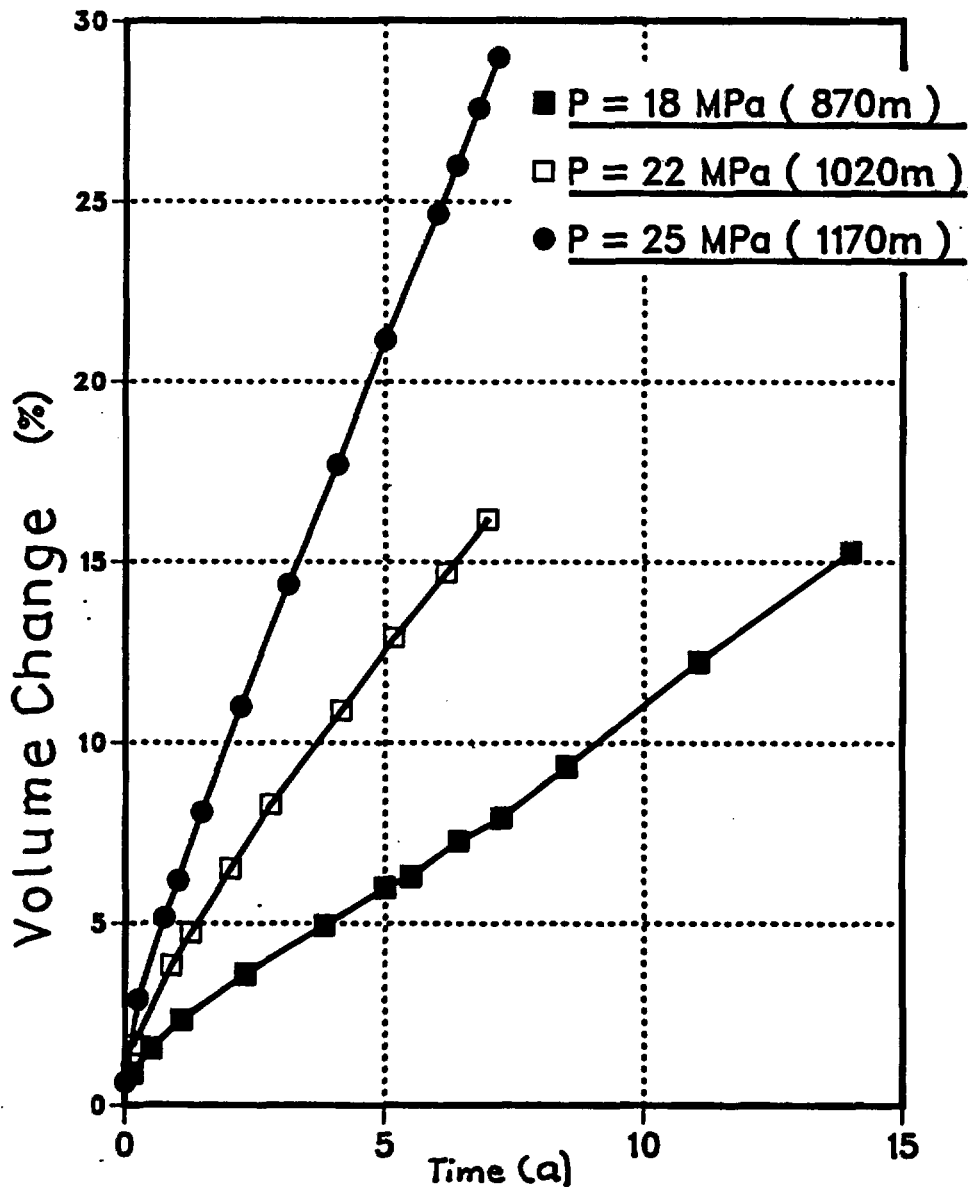


Fig. 4-4: Creep in access drift for three emplacement horizons

CONTENTS

5	EXPERIMENTAL INVESTIGATIONS	5-1
5.1	Corrosion Studies of Cask Materials	5-1
5.1.1	Objectives and Schedule	5-1
5.1.2	Ongoing Work	5-1
5.1.3	Future Work	5-4
5.2	Retention of Gaseous Fission Products in the Backfill Material	5-5
5.2.1	Objectives and Schedule	5-5
5.2.2	Ongoing Work	5-6
5.2.3	Future Work	5-6
5.3	Leaching Behavior of LWR Fuel	5-7
5.3.1	Objectives and Schedule	5-7
5.3.2	Ongoing Work	5-7
5.3.3	Future Work	5-8

5 EXPERIMENTAL INVESTIGATIONS

5.1 Corrosion Studies of Cask Materials

5.1.1 Objectives and Schedule

For qualification of the repository casks with respect to their barrier function also under the conditions of a postulated accident involving the influx of corrosive brine, extensive corrosion studies need to be conducted. The behavior of pure Hastelloy C4 material, which has been planned for use to provide corrosion protection of the POLLUX cask, is being studied under the responsibility of DWK.

In addition, further studies have been initiated at KfK/INE to determine the long-term corrosion behavior of a Hastelloy C4 surface welded coating in the combination of materials typical of POLLUX. In order to obtain additional information about the corrosion behavior of the cask shielding, also the corrosion kinetics of nodular cast iron is being studied, in less depth, in addition to Hastelloy C4.

The studies on Hastelloy C4 and nodular cast iron are being conducted in the period between 1986 and 1990.

Corrosion studies performed so far /KfK-Report 4452, 1989/ revealed a susceptibility of Hastelloy C4 to local corrosion in highly concentrated $MgCl_2$ -brines.

Therefore investigations on the suitability of steel as an improved overpack material will be carried out. In the case of its suitability the long-term corrosion protection of the disposal cask could be assumed by a self-shielding overpack with tight-welded lid and sufficiently thick wall.

Investigations on steel will take place from 1990 to 1992.

5.1.2 Ongoing Work

In order to study the influence of the thermally released salt impurity H_2S on the corrosion behavior of surface welded Hastelloy C4, specimens of a typical surface weld are investigated in a repository-relevant $NaCl$ -brine with a concentration of H_2S of 25 mg/l. This concentration value was adopted under

the assumption that the backfill material (about 1,600 m³ crushed salt per drift) releases its H₂S homogeneously (12 g/m³ salt) into 700 m³ of brine (maximum brine quantity in a drift assuming an initial backfill porosity of 30%). The testing temperature was set at 150°C, the immersion time periods are 2, 6, 12 and 18 months. The brine had a NaCl-concentration of 25,9 wt.% with little additions of MgSO₄, CaSO₄ and K₂SO₄.

Parallel to these long-term corrosion tests also hot rolled Hastelloy C4 is being investigated for comparison, either in H₂S-free and in H₂S-doped brine.

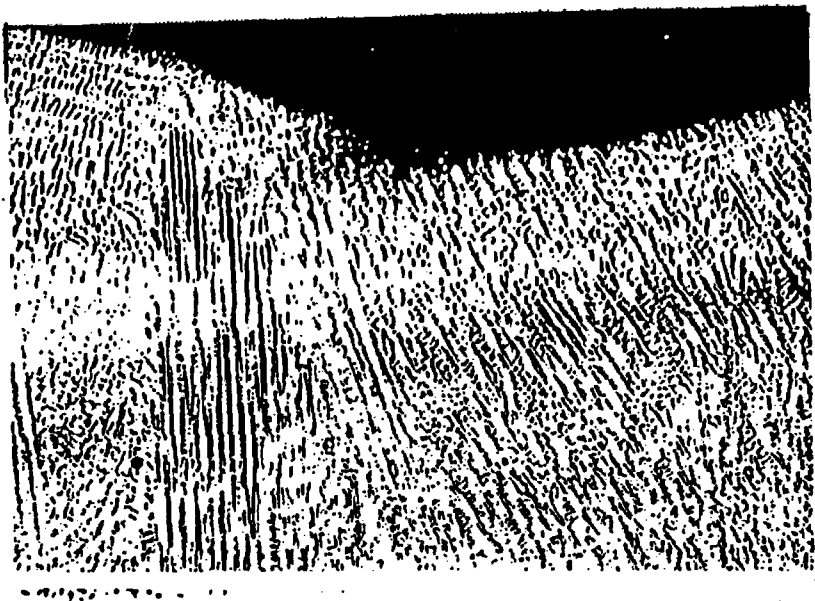
The corrosion results obtained so far with the two-months specimens (1st test series) in brine with and without H₂S have already been reported about /AE-Report No. 22E/. During the period under review the second and third test series (6 and 12 months immersion time in brine) were completed, and subsequently the samples were examined with regard to surface and local corrosion effects by gravimetry, roughness measurements (surface profiles), profilometry and metallography.

The results of the corrosion experiments on Hastelloy C4 are summarized in table 5.1-1. For comparison also results of the former 2-months experiments are included. The given integral corrosion rates are average values of two samples. Figure 5.1-1 shows micrographs of Hastelloy C4 after one year immersion time in H₂S-doped brine at 150°C.

Material conditions	Immersion time (month)	Average corrosion rate (µm/a)		Maximum depth of attack of pitting corrosion (µm)	
		NaCl-brine	NaCl-brine + 25 mgH ₂ S/l	NaCl-brine	NaCl-brine + 25 mgH ₂ S/l
surface welded	2	0,12 ± 0,02	0,91 ± 0,57	-	130
	6	0,05 ± 0,01	0,25 ± 0,02	-	20
	12	0,07 ± 0,03	0,51 ± 0,4	-	200
hot rolled	2	1,5 ± 0,24	0,87 ± 0,67	-	-
	6	1,2 ± 0,22	0,25 ± 0,02	-	-
	12	0,28 ± 0,04	0,51 ± 0,4	-	-

- = uniform surface corrosion

Table 5.1-1: Corrosion on Hastelloy C4 in NaCl-brine with and without addition of H₂S at 150°C



x 100

a)



x 100

b)

Fig. 5.1-1: Micrographs of surface welded (a) and hot rolled (b) Hastelloy C4 after 1 year exposure to NaCl-brine with 25 mg H₂S/l at 150°C

The corrosion results so far obtained on Hastelloy C4 in salt brine at 150°C can be summarized as follows:

- In NaCl-solutions free of H₂S Hastelloy C4 turned out to be highly corrosion resistant in both cases, surface welded and hot rolled. Its corrosion rates after one year immersion time were low and the material remained free of local corrosion attacks.
- Also in H₂S-doped NaCl-solution (25 ml H₂S/l) both materials showed low surface corrosion rates of 0,2 µm/a and 0,5 µm/a, respectively. Moreover, in the case of hot rolled material no local corrosion attacks could be observed, except for a slightly irregular surface corrosion. The surface welded specimens, however, showed pitting corrosion with depths of attack of up to 200 µm/a.

5.1.3 Future Work

- Completion of experiments on the influence of H₂S on the corrosion of Hastelloy C4 by post-corrosion investigation of the 18-months specimens with respect to corrosion attacks.
- Beginning of long-term corrosion tests of steel in salt brines.

5.2 Retention of Gaseous Fission Products in the Backfill Material

5.2.1 Objectives and Schedule

The project serves to study the retention capability for radioactive gases of loose and compacted salt packings. The test temperatures are 48°C and 200°C. The radiotracer technique is to be employed to determine the retention capability for the CO₂, CO, CH₄ (all C-14), HT, HTO, I₂-131, CH₃I-131, and Kr-85 gases in column tests. The retardation factors and effective diffusion coefficients are to be determined to describe the retention capability.

The study, which is being carried out by Siemens/KWU for the PtUB/SN Project Management Staff, at the Karlsruhe Nuclear Research Center, will follow the timetable set forth below (fig. 5.2-1).

Working step	1987												1988												1989											
	J	F	M	A	M	J	J	A	S	O	N	D	J	F	M	A	M	J	J	A	S	O	N	D	J	F	M	A	M	J	J	A	S	O	N	D
Preliminary tests																																				
Grain size, humidity																																				
Conversion of equipment, 200°C																																				
Analysis of mine atmosphere																																				
Iodine preparation																																				
Final granularity																																				
Influence of gas composition at 48°C																																				
at 200°C																																				
Final Carrier gas for 48°C																																				
for 200°C																																				
Isotope exchange behavior at 200°C																																				
Main experiments																																				
48°C experiments																																				
200°C experiments																																				
Final report																																				

Fig. 5.2-1: Timetable of the laboratory tests conducted to determine the retention capability of salt

5.2.2 Ongoing Work

The retardation experiments at 200°C were completed. I₂-131, CH₃I-131 and HTO were used as indicators either in loose and in consolidated salt beds (porosity E = 0,46 and 0,2). The measurement results on retardation factors and diffusion coefficients are summarized in table 5.2-1.

Indicator	Velocity of flow cm/s	Porosity	Retardation factor R	Diffusion coefficient D cm ² /s
I ₂ -131	1,2	0,46	1,3	0,6
	1,0	0,20	230	31
	1,0	0,20	1,5	0,5
	1,1	0,20	1,6	0,6
CH ₃ I-131	1,2	0,46	1,4	0,6
	1,0	0,20	1,6	0,6
HTO	1,1	0,46	20	33
	1,1	0,20	93	4,5
	2,1	0,20	40	30
	0,5	0,20	51	3,7

Experimental Conditions: Column height 40 cm
 Diameter 4 cm
 Carrier gas air

Table 5.2-1: Results of Retardation Experiments at 200°C

As result of the retardation experiments one can summarize that, except for iodine and HTO no retention was found on salt. The iodine activity retained on salt seems to depend on the iodine concentration in the carrier gas. For HTO at 200°C a better retention was found for consolidated than for loose salt beds.

5.2.3 Future Work

The formerly intended measurements are completed. Further experiments in this field are not planned for the near future.

5.3 Leaching Behavior of LWR Fuel

5.3.1 Objectives and Schedule

The project is conducted to determine the leaching resistance of spent nuclear fuel under conditions of direct disposal in salt formations. This will establish an experimental basis for modelling the source term associated with activity releases from nuclear fuels, with the accident being postulated that brine has access to the fuel elements in the repository.

The leaching experiments are being run in the hot cells of KfK in the period 1986-1992 and evaluated by the INE and IRCh institutes.

5.3.2 Ongoing Work

So far leaching experiments on spent UO_2 -fuel (52.000 MWd/t burn up) were carried out with total exposure times of up to 550 days. Figure 5.3-1 shows the results in % of the initial inventory. These data can be interpreted only by use of the non-linear thermo-dynamics of non-equilibria. It says that

- the fuel, due to its fabrication kinetic, tends to increased energy absorption during irradiation, and
- hence follows inevitably a high initial leaching rate.

Moreover, such data analysis shows that continued leaching cannot result in a considerable increase of the presented data as the surfaces, just due to the strong initial leaching, are more and more passivated.

Figure 5.3-2 shows that each nuclide at the beginning of the leaching process went into solution with its own kinetic, and afterwards went into solution congruently following a common kinetic. Two facts can be identified:

- The stronger the initial leaching rate of a nuclide, the earlier it slows down. (The data of uranium are scaled down by a factor of 100 in the figure!).

- **Congruent leaching occurs only during interim equilibria (nearly horizontal plateaus of the data).**

Finally, figure 5.3-3 presents the leached nuclide fractions in a concentration scale.

As a conclusion one can say that the leaching data of a more gross grained fuel would be lower by orders of magnitude after irradiation at higher power rates and lower burnup than those presented here. On the other side it can be expected that the actual fuel conditions will hardly change by further leaching. Further leaching fractions will approach the thermodynamic equilibrium after an infinite time period.

5.3.3 Future Work

Continuation of leaching experiments.

% of inventory

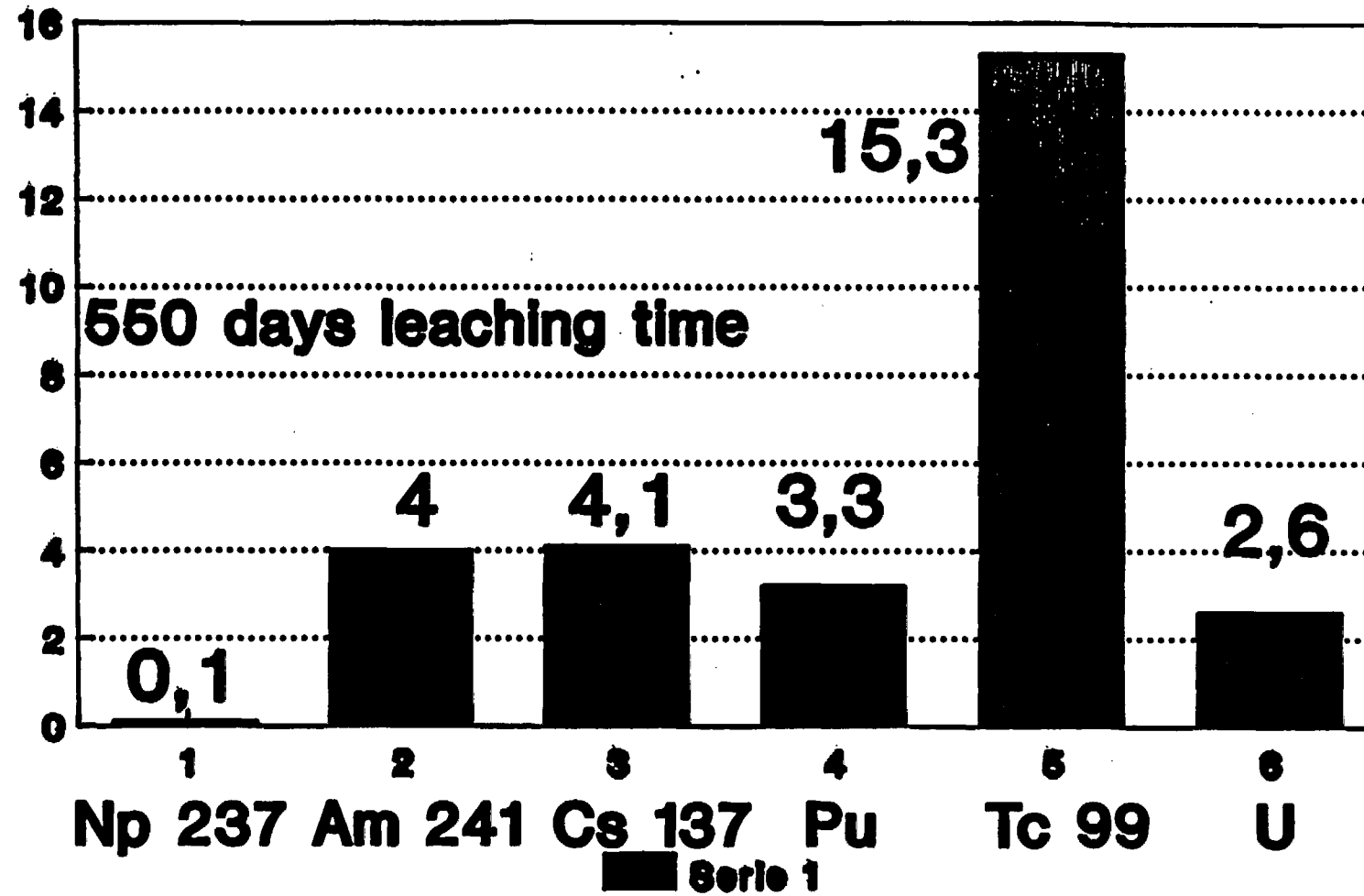


Fig. 5.3-1: Cumulated leached fractions of individual nuclides of UO₂-fuel at 52,000 MWd/t burnup

x1E-6 mol/l

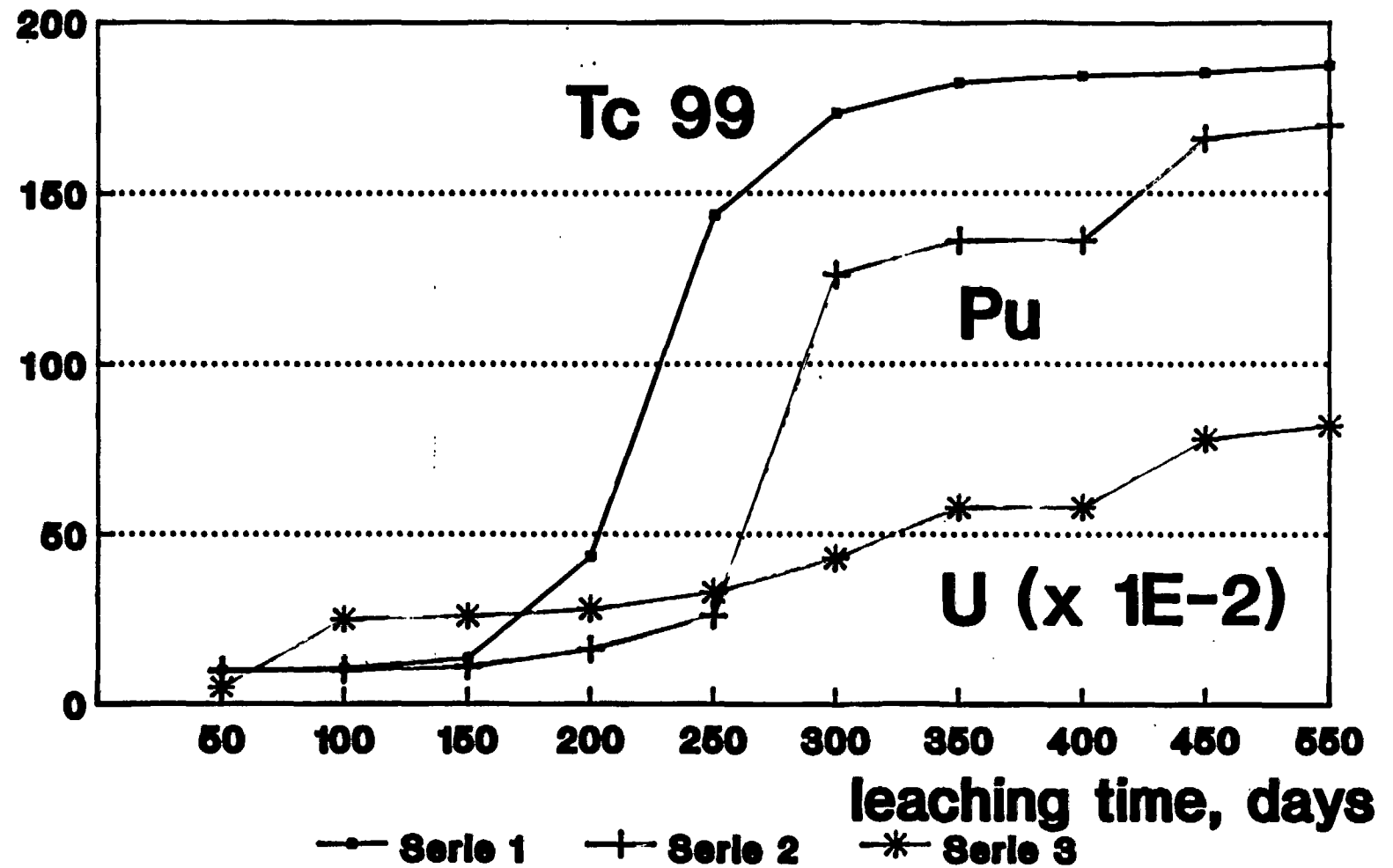


Fig. 5.3-2: Cumulated fractions of U, Pu and Tc-99 of UO₂-fuel

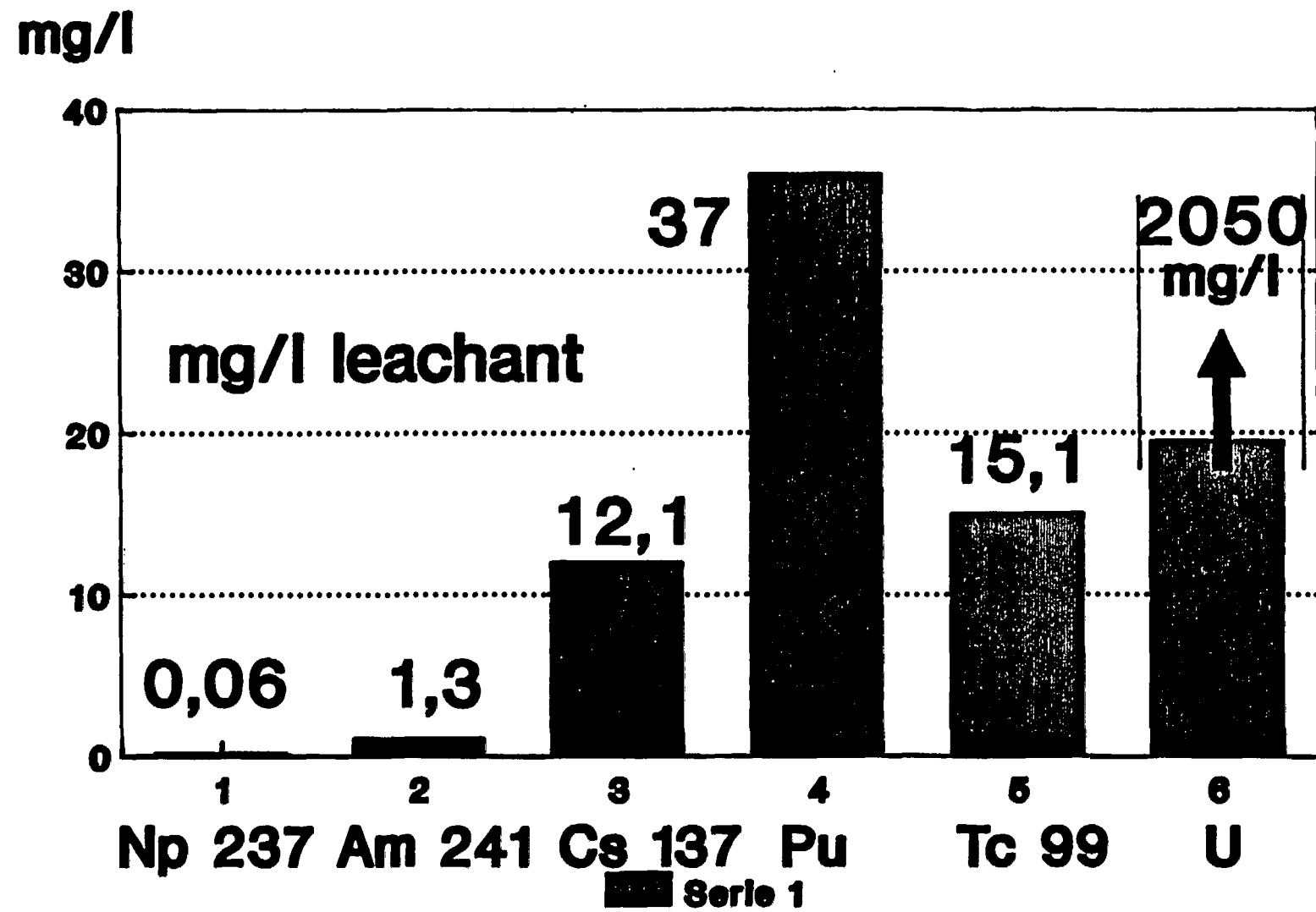


Fig. 5.3-3: Nuclide concentration after 550 days leaching time

CONTENTS

6 REFERENCES 6-1

6 REFERENCES

- /3-1/ Pahl,A. et al.: Geotechnisches Verhalten verschiedener Salzgesteine-Teilprojekt III: In-situ-Meßtechnik im Salz. Schlußbericht zum BMFT-Forschungsvorhaben KWA 5502 8, Archiv-Nr. 103538, BGR, Hannover, 1988.
- /3-2/ Langer,M.; Liedtke,L.&Pahl,A.: Felshydraulische Tests zur Bestimmung der Barrierewirkung von geklüftetem Fels. Mitteil. Ing. u. Hydrogeol., 32: 467-484, Aachen, 1989.
- /3-3/ Institut für Strömungsmechanik und Elektron. Rechnen im Bauwesen: DURST (Durchströmung und Transport in klüftigem Gestein) - GM88 (Gasmmodell). Universität Hannover, 1989.
- /3-4/ Liedtke,L.&Naujoks,A.: Bohrlochkranzversuche (Fracture System Flow Test) - Felslabor Grimsel. Jahresbericht zum BMFT-Forschungsvorhaben KWA 3504 A5, BGR, Hannover, 1989.
- /3-5/ Vogt,H.G.: Streustrahlungsrechnungen für Neutronen in Salzstollen, Auftrag KfK 315 I02847580I 0934, 1989
- /3-6/ Cohlen, M.O. et al: SAM-CE, A Monte-Carlo-code for neutron, gamma ray and electron transport, Rev. 5, Mathematical Applications Group, Inc, MR 7052-5, 1977
- /4-1/ PAE-Halbjahresbericht, 01.01.1987-30.06.1987, AE-Nr. 19
- /4-2/ PAE-Halbjahresbericht, 01.07.1987-31.12.1987, AE-Nr. 20
- /4-3/ Commission of the European Communities, Hrsg. Lowe, M.J.S. and Knowles, N.C. COSA II-Further benchmark exercises to compare geomechanical computer codes for salt, final report, EUR 12135 (1989)

/4-4/ Dietmann N., Hunsche U., Meister D. „Über das geomechanische Verhalten von Steinsalz bei erhöhten Temperaturen“, Z.d.t. geol. Ges., Band 137, S. 29-46 (1986)

/4-5/ PAE-Halbjahresbericht, 01.01.1988-30.06.1988, AE-Nr. 21

CONTENTS

7 ABBREVIATIONS AND ACRONYMS 7-1

7 ABBREVIATIONS AND ACRONYMS

Oc	Degrees Centigrade
AET	NUKEM/DWK-Project „Andere Entsorgungstechniken“ (1981-1984)
AVR	Arbeitsgemeinschaft Versuchsreaktor; German pebble-bed research reactor
BfS	Bundesamt für Strahlenschutz; Federal Office for Radiation Protection, Germany
BGR	Bundesanstalt für Geowissenschaften und Rohstoffe; Federal Institute of Geosciences and Natural Resources, Germany
BMFT	Bundesministerium für Forschung und Technologie; Ministry for Research and Technology, Germany
BWR	Boiling Water Reactor
cm	Centimeter
DBE	Deutsche Gesellschaft zum Bau und Betrieb von Endlagern für Abfallstoffe mbH; German Repository Company
DD	Direct Disposal
DIN	Deutsche Industrie-Norm; German Industrial Standard
DWK	Deutsche Gesellschaft für Wiederaufarbeitung von Kernbrennstoffen mbH; German Reprocessing Company
FBR	Fast Breeder Reactor
GNS	Gesellschaft für Nuklear-Service GmbH; Company for Nuclear-Service
GSF	Gesellschaft für Strahlen- und Umweltforschung; Company for Radiation and Environmental Research, Germany
GWd	Gigawatt-day
HM	Heavy Metal
HTR	High-Temperature Reactor
INE	Institut für Nukleare Entsorgungstechnik; KfK's Institut for Nuclear Entsorgung
IRCh	KfK's Radiochemistry Institute

kN	Kilonewton
kW	Kilowatt
KfK	Kernforschungszentrum Karlsruhe; Karlsruhe Nuclear Research Center, Germany
KWU	Kraftwerk-Union; Power Plant Union
l	Liter
LMFBR	Liquid-Metal Fast Breeder Reactor
LWR	Light-Water Reactor
m	Meter
MOX	Mixed-Oxide
MPa	Megapascal; 1 MPa = 10 bar
MWd	Megawattday
PtUB/SN	Projektträgerschaft Universitätsforschung zum nuklearen Brennstoffkreislauf/Stilllegung von Nuklearanlagen; Group for Coordination of Fuel-Cycle-Related R + D Work at Universities
PAE	Projektgruppe Andere Entsorgungstechniken; Project Group "Direct Disposal" at KfK
PWR	Pressurized Water Reactor
R + D	Research and Development
t	ton (metric ton)
TÜV	Technischer Überwachungsverein; Germany's Independent Technical Supervising Authority
THTR	Thorium High-Temperature Reactor
yr	year